

Structural changes to forests during regeneration affect water flux partitioning, water ages and hydrological connectivity: Insights from tracer-aided ecohydrological modelling

Aaron J. Neill¹, Christian Birkel^{2,1}, Marco P. Maneta^{3,4}, Doerthe Tetzlaff^{5,6,1}, Chris Soulsby¹

¹ Northern Rivers Institute, University of Aberdeen, Aberdeen, United Kingdom.

² Department of Geography, University of Costa Rica, San Pedro, Costa Rica.

³ Geosciences Department, University of Montana, Missoula, MT, USA.

⁴ Department of Ecosystem and Conservation Sciences, W.A Franke College of Forestry and Conservation, University of Montana, Missoula, MT, USA.

⁵ Department of Ecohydrology, IGB Leibniz Institute of Freshwater Ecology and Inland Fisheries, Berlin, Germany.

⁶ Department of Geography, Humboldt University of Berlin, Berlin, Germany.

Correspondence to: Aaron J. Neill (aaron.neill@abdn.ac.uk)

Abstract. Increasing rates of biodiversity loss are adding momentum to efforts seeking to restore or rewild degraded landscapes. Here, we investigated the effects of natural forest regeneration on water flux partitioning, water ages and hydrological connectivity, using the tracer-aided ecohydrological model EcH₂O-iso. The model was calibrated using ~3.5 years of diverse ecohydrological and isotope datasets available for a catchment in the Scottish Highlands, an area where the impetus for native pinewood regeneration of native pinewoods is growing. We then simulated two land cover change scenarios were simulated that incorporated forests at early (dense thicket) and late (old open forest) stages of regeneration, respectively, and compared these to a present-day baseline simulation. Changes to forest structure (proportional vegetation cover, vegetation heights and leaf area index of pine trees) were modelled for each stage. The scenarios were then compared to a present-day baseline simulation. Establishment of thicket forest had substantial the greatest ecohydrological consequences for the catchment. Specifically, effect on water partitioning/ages and connectivity, with increased losses to transpiration and, in particular, interception evaporation drove ~~iving~~ reductions in below-canopy fluxes (soil evaporation, groundwater- (GW) recharge and streamflow) and generally slower rates of water turnover. Greatest reductions in streamflow and connectivity were simulated for summer baseflows and small to moderate events during summer and the autumn/winter rewetting period. This resulted from the effect of local changes to flux partitioning in regenerating areas on the hillslopes extending to the wider catchment by reducing downslope GW subsidies that help sustain summer baseflows and saturation in the valley bottom. Meanwhile, Effects on streamflow were most evident for low and moderate summer flows rather than winter higher flows were relatively less affected, especially in winter. Whilst full forest regeneration was limited to hillslopes, resultant changes to the spatial dynamics of flux partitioning could also cause drying out of the valley bottom. Despite the generally drier state of the catchment, simulated water ages suggested that the increased transpiration demands of the thicket forest could be satisfied by moisture carried over from previous seasons. The more open nature of the older forest generally resulted in water

Formatted: Font color: Auto

Formatted: Font color: Auto

fluxes, water ages and connectivity ~~characteristics~~—returning towards baseline conditions. Our work implies that the ecohydrological consequences of natural forest regeneration ~~on degraded land~~ depend on the structural characteristics of the forest at different stages of ~~development~~development.—Consequently, future land cover change investigations need to move beyond consideration of simple forest vs. non-forest scenarios to inform sustainable management that effectively balances landscape restoration efforts with demand for ecosystem services. ~~Tracer-aided ecohydrological models were also shown to be useful tools for land cover change simulations and further potential of such models was highlighted.~~

1 Introduction

Increasing rates of biodiversity loss and ecosystem degradation have highlighted the urgent need for landscape conservation and restoration (Rands et al., 2010). Unlike approaches seeking to retain sets of predetermined characteristics, rewilding takes a relatively “hands-off” approach to restoration by seeking to restore dynamic natural processes that create self-sustaining, complex ecosystems (Navarro and Pereira, 2015; Perino et al., 2019). The Scottish Highlands represent a degraded landscape for which rewilding is increasingly promoted as a means of restoring native pinewoods that have been lost due to human land management practices (~~Deary and Warren, 2017~~; zu Ermgassen et al., 2018). Following the last glaciation, the dominant vegetation over much of the Highlands was open forests dominated by Scots Pine (*Pinus sylvestris*) and birch (*Betula* spp.) (Steven and Carlisle, 1959). Today, however, such native pinewoods cover only ~1% of their Holocene maximum extent (Mason et al., 2004). This is largely due to~~However,~~ industrial exploitation in the 17-19th centuries, and interruption of natural regeneration due to intensification of sheep grazing and management of Highland estates for deer and grouse shooting since the mid-19th century (Steven and Carlisle, 1959; Wilson, 2015~~;~~). Competing perspectives may exist on the overall trajectory rewilding initiatives should take which, in turn, will affect the final characteristics of restored native pinewoods (c.f. Deary and Warren, 2017). In any event, however, a central requirement is that the process of natural forest regeneration be restarted through reduction of grazing pressures and establishment of new seed sources via targeted tree planting; this will~~means that remaining native pinewoods now cover only ~1% of their Holocene maximum extent (Mason et al., 2004). The goal of rewilding in the Highlands would be to restore the process of natural forest regeneration through initial human interventions to reduce grazing pressures and establish new seed sources through targeted tree planting;~~ ultimately lead ing to the proliferation and maintenance of self-sustaining native pinewoods (Thomas et al., 2015; zu Ermgassen et al., 2018).

Vegetation plays a crucial role in partitioning land-surface water and energy fluxes, whilst soil moisture determines water availability for root uptake and plant growth (Rodriguez-Iturbe, 2000), and determines the water-limited edge of forest extents (Simeone et al., 2018). Therefore, elucidating the potential ecohydrological consequences of natural forest regeneration is crucial for sustainable land management and for understanding how land cover change may affect other ecosystem services. This is relevant beyond Scotland as reforestation is widely seen as a means of reducing flood and erosion risks, improving water quality, and mitigating climate change (Bonan, 2008; Chandler et al., 2018; Ellison et al., 2017; Iacob et al., 2017; Rudel

65 et al., 2020). Of particular importance is how partitioning of water between “blue” (i.e. groundwater (GW) recharge and stream
discharge) and “green” (i.e. evapotranspiration (ET)) fluxes is affected in space and time, as this has implications for water
availability to terrestrial and aquatic ecosystems, and downstream water users (Falkenmark and Rockström, 2006; 2010). In
addition, consideration of water ages and the spatio-temporal dynamics of hydrological connectivity can reveal how storage-
flux dynamics and hydrological source areas are affected by regeneration (Bergstrom et al., 2016; Kuppel et al., 2020; Tetzlaff
70 et al., 2014; Sprenger et al., 2019). This has implications for ecosystem resilience to climatic extremes (Fennell et al., 2020;
Kleine et al., 2020; Smith et al., 2020), generation of low/high flows (Birkel et al., 2015; Nippgen et al., 2015), and
redistribution of water and solutes (Bergstrom et al., 2016; Turnbull and Wainwright, 2019).

Previous work investigating the hydrological consequences of forest (re)generation has often employed the paired-catchment
75 approach to assess how changes in forest cover affect aggregated metrics (e.g. water balance and water yield) that characterise
catchment functioning (Bosch and Hewlett, 1982; Brown et al., 2005; Filoso et al., 2017). However, findings from such studies
may be biased as many only consider the early stages (~first 10 years) of forest development, often within the context of
commercial (possibly non-native) plantation management (Coble et al., 2020; Ellison et al., 2017; Filoso et al., 2017). Where
long-term sites have been established, data have indicated that age-related changes to forest structure and tree physiology can
80 substantially influence water partitioning (Coble et al., 2020; Marc and Robinson, 2007; Perry and Jones, 2017; Scott and
Prinsloo, 2008; Segura et al., 2020). However, the focus on commercial plantations, especially so in the UK context (Marc and
Robinson, 2007), may limit transferability of findings to scenarios of passively managed natural forest regeneration associated
with rewilding. In particular, forest harvesting cycles (~40 years) are much shorter than the lifespan (>150 years) of trees in
natural forests (Brown et al., 2005; Ellison et al., 2017; Summers et al., 2008), whilst plantation management practices (e.g.
85 drainage, species selection, thinning, etc.) may confound effects of land cover change (Birkinshaw et al., 2014; Robinson,
1998). Along with general drawbacks to the paired-catchment approach (e.g. limited ability to resolve spatio-temporal changes
to internal catchment processes; Brown et al., 2005), these factors demonstrate the need to better understand the
ecohydrological consequences of a naturally regenerating forest, using methods that can disaggregate the drivers of aggregated
catchment responses in space and time.

90 Spatially distributed ecohydrological models explicitly simulate the tight coupling of water, energy, and vegetation dynamics
in time and space (Faticchi et al., 2016a). Consequently, they are promising tools for investigating the ecohydrological impacts
of land cover change (Ellison et al., 2017; Manoli et al., 2018; Peng et al., 2016). Models are also advantageous in providing
a virtual, controlled environment within which different scenarios of land cover change can be simulated and compared against
95 a baseline (Du et al., 2016). A critical prerequisite to using ecohydrological models is confidence in accurate representation of
internal catchment functioning (Seibert and van Meerveld, 2016). ~~Given that the i~~Integration of stable water isotope tracers
($\delta^2\text{H}$ and $\delta^{18}\text{O}$) within models can have significant value in this regard through helping to constrain storage and mixing volumes
necessary to simultaneously capture the celerity (discharge) and velocity (flow paths and connectivity) responses of catchment

100 systems (Birkel and Soulsby, 2015; McDonnell and Beven, 2014). This has been demonstrated for both conceptual models (e.g. Birkel et al., 2011) and more complex, spatially-distributed models (e.g. Holmes et al., 2020). Consequently, the tracer-aided ecohydrological model EcH₂O-iso has recently been developed (Kuppel et al., 2018a). EcH₂O-iso has successfully been applied to a range of environments to elucidate links between land cover and water partitioning/ages (e.g. Douinot et al., 2018; Gillefalk et al., 2021; Knighton et al., 2020; Kuppel et al., 2020; Smith et al., 2019; 2020).

105 Here, we applied EcH₂O-iso to a small experimental catchment in the Scottish Highlands to investigate the ecohydrological consequences of natural pinewood regeneration on degraded land. Specifically, we compared a present-day baseline simulation with two land cover change scenarios that incorporated forests at early (dense thicket) and late (old open forest) stages of regeneration, respectively. Changes to forest structure (proportional vegetation cover, vegetation heights and leaf area index (LAI) of pine trees) were modelled for each stage. Soil properties were held constant as uncertainty surrounds it is unclear how “effective” parameters describing their aggregated characteristics respond to land cover change (Seibert and van Meerveld, 2016). Furthermore, the effect of conifer forests can have inconsistent effects on soil properties; can be unclear, as soil acidification from needle decomposition may compete with improvements to soil structure caused by increases in organic matter and root density (Archer et al., 2013; Chappell et al., 1996). The wet and windy climate of Scotland also makes it likely that changes in canopy structure and interception losses will predominantly determine variations in water partitioning (c.f. Farley et al., 2005; Marc and Robinson, 2007). Our specific objectives were to evaluate the effect of forest structure at different stages of regeneration stage on:

1. Dynamics of water flux partitioning in time and space,
2. Ages of “blue” and “green” water fluxes,
- 120 3. Hydrological connectivity under contrasting flow conditions.

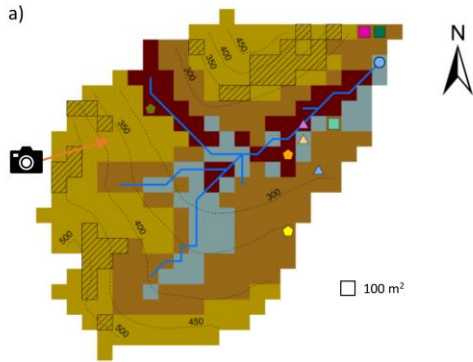
2 Study site

The Bruntland Burn (BB) catchment (3.2 km²) is in the Cairngorms National Park in the Scottish Highlands (Fig. 1a). It is a tributary of the Girnock Burn catchment (31 km²) that drains into the River Dee. The Dee supports a globally important Atlantic Salmon-salmon (*Salmo salar*) population and provides drinking water to over 300,000 people (Langan et al., 1997; Soulsby et al., 2016). The glacial legacy of the BB-catchment has left steep hillslopes and a flat valley bottom. Bedrock is mostly granite with schists and other metamorphic rocks fringing the catchment. This is overlain by extensive drift deposits (70% of catchment area) that are 5-10 m deep on lower hillslopes and up to 40 m deep in the valley bottom (Soulsby et al., 2016). Peat (up to 4 m deep) and peaty gley soils overlay the deeper drift deposits with peaty podzols and poorly developed rankers characterising higher elevations along with some bedrock outcrops (Fig. 1a).

Formatted: Font: Italic

135 Natural Scots pine regeneration is restricted due to grazing from high densities of red deer (*Cervus elaphus*; 11 to 14.9 deer km⁻² (SNH, 2016)) and controlled burning of grouse moorlands. Consequently, tree cover is largely limited to native pinewoods on the relatively inaccessible steep northern hillslope and pine plantations at the catchment outlet (Figs. 1 and 2a+b-e). Vegetation otherwise reflects soil type; heather (*Calluna vulgaris*, *Erica tetralix*) dominates the peaty podzols and rankers of the hillslopes (Fig. 1d), whilst *Molinia* grassland on the peaty gleys (Fig. 1f) is increasingly outcompeted by *Sphagnum* spp. on the waterlogged peats of the valley bottom (Fig. 2a+e). Isolated pine trees are scattered throughout the catchment, with those in the wetter valley bottom exhibiting stunted growth (“Bog pine” in Fig. 2a)–Fig. 1g).

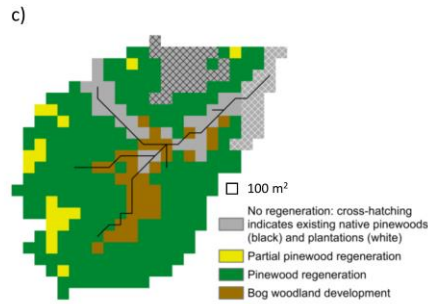
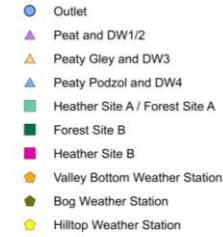
140 Mean annual precipitation is 1000 mm and potential evapotranspiration are 1000 mm and is 400 mm, respectively, with the former usually fallings in low-intensity events (<10 mm d⁻¹). Less than 5% of precipitation falls as snow, reflecting as mean temperatures ranging between 1 °C in winter and 13 °C in winter and in summer, respectively. Seepage of fracture flow from bedrock outcrops and shallow sub-surface flow through the rankers predominantly move vertically on reaching the podzols to recharge stores of groundwater (GW) in the underlying drift (Blumstock et al., 2016; Tetzlaff et al., 2014) which sustain baseflow conditions in the stream (Blumstock et al., 2015). The storm response of the BB is non-linear, depending on the
145 dynamic expansion of the riparian saturation area which generates overland flow and hydrological connectivity between the hillslopes and valley bottom (Birkel et al., 2015; Soulsby et al., 2015).



Soil Type



Monitoring Site



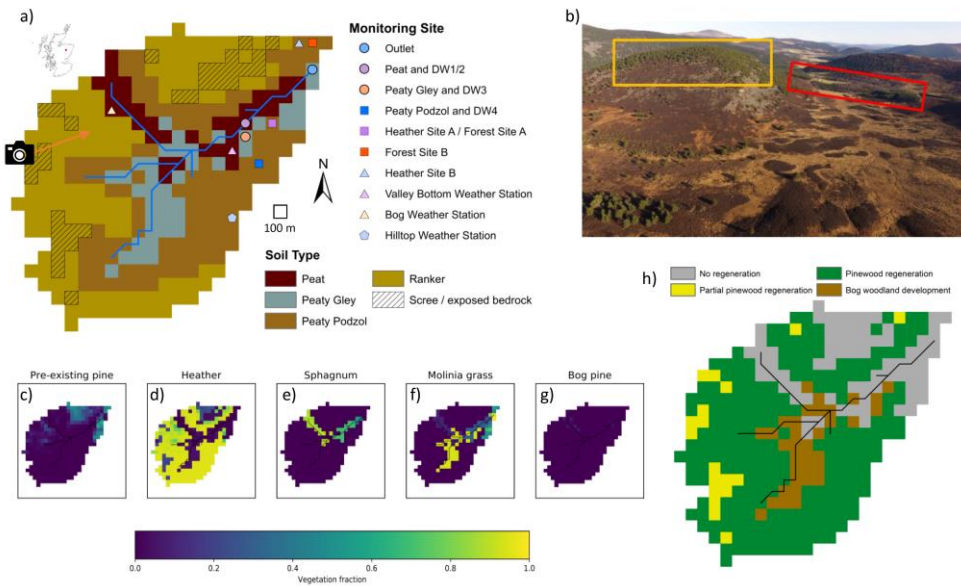


Figure 1: Characteristics of the Bruntland Burn catchment: a) Map showing distribution of soil types and monitoring sites (DW = Deeper groundwater Well) and elevation contours; b) Aerial view showing current distribution of vegetation types in the catchment - yellow and red boxes show areas of established natural forest and land managed for plantations, respectively, whilst direction of the photo is shown by the arrow in a); c-g) Present-day vegetation coverage in the catchment (as also used in the baseline scenario simulation); h) Map of regeneration potential (Partial pinewood regeneration signifies areas where regeneration is limited due to presence of scree/exposed bedrock). Photo in b) by Aaron J. Neill.

3 Methods

3.1 The EcH₂O-iso model

EcH₂O-iso is a development of the ecohydrological model EcH₂O (Maneta and Silverman, 2013). It consists of three tightly coupled modules simulating the water balance, vertical energy balance and vegetation growth dynamics, and an additional fourth module that tracks the stable water isotope composition and ages of hydrological stores and fluxes (Kuppel et al., 2018a).

The model domain is defined by a regularly gridded digital elevation model (DEM) that sets local flow directions, and

governing equations are solved for fixed timesteps using finite-differences. Proportional coverages of different vegetation types (based on physiology and structure) and bare soil are specified for each grid cell.

The energy balance is resolved sequentially for the canopy and soil surface. ~~Canopy temperature is determined iteratively to balance H_l latent (due to transpiration and evaporation of intercepted water) and sensible heat fluxes depend on canopy temperature; this is determined iteratively such that latent and sensible heat fluxes balance with~~ net radiation reaching the canopy. Interception evaporation is limited by available intercepted water whilst a Jarvis-type stomatal conductance model limits transpiration. Transpiration demand is satisfied by root water uptake from three soil layers (L1 -3, with L1 being the topmost layer), L2 and L3) with calibrated depths, in proportion to the water content and fraction of roots in each layer. ~~A n exponential function determines the latter. The latter is determined by an exponential function describing how root fraction decreases with depth~~ (Kuppel et al., 2018b). At the soil surface, iteratively determined temperature partitions net radiation and heat advected by rainfall/throughfall into latent heat for snowmelt and soil evaporation from L1, sensible heat exchanges between the soil and atmosphere, and heat into the ground and snowpack. Soil evaporation is limited by the moisture content of L1. In addition to soil, two further hydrological stores are conceptualised: canopy interception storage and ponded water.

Once interception storage is full, throughfall reaches the ponded water store where it may infiltrate into L1 based on the Green-Ampt model (Mein and Larson, 1973). Vertical redistribution of water occurs via gravitational drainage when volumetric water content (VWC) in any of the soil layers exceeds field capacity. Drainage rates are proportional to the water content in the layer until they reach effective vertical saturated hydraulic conductivity. Gravitational water in L3 can leak through the bottom model boundary from the model domain or, move laterally as GW simulated via a kinematic wave model, or seep into the stream channel. The kinematic wave model assumes that L3 is parallel to the surface and therefore flow velocity is proportional to terrain slope and the horizontal effective hydraulic conductivity. The latter, along with an exponential function describing how resistance to flow across the channel-subsurface boundary varies with gravitational water depth, also controls the rate at which seepage to the stream occurs. Water remaining in ponded storage is routed to the next downslope cell as overland flow that can potentially reach the stream within one timestep if it is not reinfilted along the way ~~travel the length of the catchment to reach the stream within one timestep.~~ GW also seeps to the stream, with ~~e~~ Channel routing is simulated using a kinematic wave model. ~~Stable water H₂ isotopes and water ages are tracked assuming complete mixing (Eq. 1 in Smith et al., 2020), with isotopic fractionation due to evaporation in L1 simulated via the Craig-Gordon model (Craig and Gordon, 1965; Kuppel et al., 2018a). Vegetation growth dynamics were not simulated in this application; consequently, vegetation characteristics were static for within each considered scenario. Previous work provides~~ For further details of ECH₂O and ECH₂O-iso see (Kuppel et al., 2018a; 2018b), Maneta and Silverman, (2013) and Smith et al., (2020).

3.2 Present-day baseline scenario

Catchment soil distribution was based on major Hydrology of Soil Types (HOST) classifications (Fig. 1a; Tetzlaff et al., 2007). Soil types were assumed to be spatially uniform. The properties of each individual soil type were assumed to be spatially uniform. Five vegetation types characterised the present-day baseline scenario: Pre-existing Scots pine, heather (also used to represent other understorey shrubs such as bilberry), *Molinia* grass, *Sphagnum* and bog pine (Table 1). LiDAR-based estimates of canopy cover were used to derive proportional tree coverages in each cell (c.f. Kuppel et al., 2018b); trees on the podzols/rankers (plus those in plantations) and on the wetter peat/peaty gleys were designated as pre-existing pine (Fig. 1e) and bog pine (Fig. 1g), respectively (Fig. 2a), enabling stunted development of the latter due to waterlogging to be explicitly represented (McHaffie et al., 2002). The extents of remaining vegetation types (Table 1; Fig. 2a-d-f) were derived from the soil distribution, field mapping and aerial imagery (Kuppel et al., 2018b; Tetzlaff et al., 2007). To account for scree and exposed bedrock (Fig. 1a), some rankers on the western and northern hillslopes were set with bare earth coverages of 80% and up to 95% of the treeless surface, respectively (Fig. 1a). All vegetation heights in the baseline scenario were based on local knowledge (Table 1).

Table 1: The vegetation types considered in each scenario organised by soil type in the baseline and regeneration scenarios. All vegetation types are shown for the baseline scenario whilst only those in areas of pinewood regeneration on podzols/rankers or bog woodland development on peaty gleys are given for the regeneration scenarios (see Fig. 1c). In areas where regeneration is not possible, vegetation characteristics remain as they were in the baseline scenario. The total coverage of all vegetation types plus bare earth sum to 100% within each cell of a given soil type. Leaf area index (LAI) scale factors convert calibrated values of LAI for pre-existing pine to LAIs for thicket, old open or bog pine, along with their distribution by soil type, proportional aerial coverage, height, and leaf area index (LAI) scaling.

Scenario and soil type	Vegetation type	Proportional aerial coverage	Height (m)	LAI scale factor
<u>Baseline</u>				
Podzol & ranker	Pre-existing pine	LiDAR-derived	10	1
	Heather	95% of treeless area except in existing native pinewoods (40% of treeless area to account for rocky terrain), plantations (0%) or areas of scree/bedrock (5 to 20% of treeless area)	0.4	-
	<i>Molinia</i> grass	99% of treeless area in plantations	0.5	-
Peaty gley	Pre-existing pine	LiDAR-derived in plantations	10	1
	Bog pine	LiDAR-derived	3.4	0.17
	Heather	5% of treeless area except in plantations (0%)	0.4	-
	<i>Molinia</i> grass	99% of tree- and shrub-less area	0.5	-

Formatted: Font: Italic

Formatted: Font: Not Italic

<u>Peat</u>	<u>Pre-existing pine</u>	<u>LiDAR-derived in plantations</u>	<u>10</u>	<u>1</u>
	<u>Bog pine</u>	<u>LiDAR-derived</u>	<u>3.4</u>	<u>0.17</u>
	<u>Sphagnum</u>	<u>70% of treeless area except in north-west (90% of treeless area)</u>	<u>0.1</u>	<u>-</u>
	<u>Molinia grass</u>	<u>99% of tree- and moss-less area</u>	<u>0.5</u>	<u>-</u>
<u>Thicket forest</u>				
<u>Podzol & ranker</u>	<u>Thicket pine</u>	<u>95% of available pinewood regeneration area ^a</u>	<u>12.7 ^b</u>	<u>1.37</u>
	<u>Heather</u>	<u>9% of available treeless pinewood regeneration area ^c</u>	<u>0.12 ^c</u>	<u>-</u>
<u>Peaty gley</u>	<u>Bog pine</u>	<u>15% of available bog woodland area ^d</u>	<u>2.4</u>	<u>0.04</u>
	<u>Heather</u>	<u>75% of available treeless bog woodland area ^e</u>	<u>0.4</u>	<u>-</u>
	<u>Molinia grass</u>	<u>99% of available tree- and shrub-less bog woodland area ^e</u>	<u>0.5</u>	<u>-</u>
<u>Old open forest</u>				
<u>Podzol & ranker</u>	<u>Old open pine</u>	<u>54% of available pinewood regeneration area ^a</u>	<u>15.5 ^b</u>	<u>0.59</u>
	<u>Heather</u>	<u>82% of available treeless pinewood regeneration area ^c</u>	<u>0.29 ^c</u>	<u>-</u>
<u>Peaty gley</u>	<u>Bog pine</u>	<u>15% of available bog woodland area ^d</u>	<u>8.4</u>	<u>0.4</u>
	<u>Heather</u>	<u>75% of available treeless bog woodland area ^e</u>	<u>0.4</u>	<u>-</u>
	<u>Molinia grass</u>	<u>99% of available tree- and shrub-less bog woodland area ^e</u>	<u>0.5</u>	<u>-</u>

Notes: ^a Based on plan drawings of Thicket (Type 25) and Old open forest (Type 3) in Figure 3 of Summers et al. (1997); ^b Median height of aged trees from Thicket and Old open woodland in Table 2 of Summers et al. (2008); ^c Sum of shrub cover or cover-weighted average height of shrubs for Thicket and Old open pines in Table 1 of Parlane et al. (2006); ^d Based on pine cover in uncut bogs reported by McHaffie et al. (2002); ^e Based on field descriptions of Steven and Carlisle (1959).

Formatted: Normal

Scenario and vegetation type	Soil distribution	Cover	Height (m)	LAI scale factor-^a
<i>Baseline</i>				
<u>Pre-existing pine</u>	<u>Podzol & ranker</u>	<u>LiDAR-derived</u>	<u>10</u>	<u>1</u>
<u>Heather</u>	<u>Peaty gley</u>	<u>5% of treeless area</u>	<u>0.4</u>	<u>-</u>
	<u>Podzol & ranker</u>	<u>95% of treeless area</u>	<u>0.4</u>	<u>-</u>

		(5 to 40% of treeless area if scree or bedrock present)		
<i>Sphagnum</i>	Peat	70% of treeless area except in NW (90% of treeless area)	0.1	-
<i>Molinia</i> -grass	Peaty-gley & peat	99% of tree-, shrub- and moss-less area	0.5	-
Bog-pine	Peat & peaty-gley	LiDAR-derived	3.4	0.17
<i>Thicket woodland</i>				
Pre-existing-pine	Podzol & ranker	As-baseline in areas of present-day native pinewood and plantation	10	1
Heather	Peaty-gley	75% of available treeless bog woodland area ^b	0.4	-
	Podzol & ranker	9% of available treeless pinewood regeneration area ^c	0.12 ^c	-
		As-baseline in area of present-day native pinewood	0.4	-
<i>Sphagnum</i>	Peat	As-baseline		
<i>Molinia</i> -grass	Peat	As-baseline		
	Peaty-gley	99% of available tree- and shrub-less bog woodland area ^b	0.5	-
Bog-pine	Peaty-gley	15% of available bog woodland area ^{d,e}	2.4	0.04
	Peat	As-baseline		
Thicket-pine	Podzol & ranker	95% of available pinewood regeneration area ^f	12.7 ^f	1.37
<i>Old open woodland</i>				
Pre-existing-pine	Podzol & ranker	As-baseline in areas of present-day native pinewood and plantation	10	1
Heather	Peaty-gley	75% of available treeless bog woodland area ^b	0.4	-
	Podzol & ranker	82% of available treeless pinewood regeneration area ^c	0.29 ^c	-
		As-baseline in area of present-day native pinewood	0.4	-
<i>Sphagnum</i>	Peat	As-baseline		
<i>Molinia</i> -grass	Peat	As-baseline		
	Peaty-gley	99% of available tree- and shrub-less bog woodland area ^b	0.5	-
Bog-pine	Peaty-gley	15% of available bog woodland area ^{d,e}	2.4	0.4
	Peat	As-baseline		
Old open-pine	Podzol & ranker	54% of available pinewood regeneration area ^f	15.5 ^f	0.59

Notes: ^aWith respect to calibrated Pre-existing pine leaf area index (LAI); ^bSteven and Carlisle (1959); ^cParlane et al. (2006); ^dMcHaffie et al. (2002); ^eSummers (2018); ^fSummers et al. (1997); ^gSummers et al. (2008).

3.3 Baseline calibration

220 The baseline scenario was simulated from 21 February 2013 to 08 August 2016 on a 100 m×100 m grid with a daily timestep. Model forcing data are detailed in [Supplementary Table S1](#). Six years of looped data were used to spin-up the model for calibration whilst 30 years were used for post-calibration runs to stabilise water ages (c.f. Kuppel et al., 2020). Calibration followed a Morris sensitivity analysis (Morris, 1991; Sohler et al., 2014) to identify sensitive parameters (Table S2). For efficiency, it was assumed that pre-existing pine and bog pine vegetation types could take the same parameter values except for *leaf-area-index (LAI)* (*italics signify parameter name*); thus, only four sets of vegetation parameters required calibration. Overall, 90 parameters (10 × 4 for soil, 12 × 4 for vegetation and 2 for [stream channel](#)) were calibrated. The parameter space was sampled by conducting 100,000 Monte Carlo simulations. Parameter values were drawn from initial ranges informed by Kuppel et al. (2018b) and additional literature reviews (Table S2). The LAI of bog pine was related to the sampled LAI of pre-existing pine via a scale factor accounting for relative differences in canopy architecture. The scale factor (0.17) ~~was equalled~~ 225 the ~~proportional difference between~~ an empirical estimate of LAI for bog pine ~~and was of~~ a local measurement of LAI for Scots pine (Wang et al., 2018). The former was obtained by first estimating [the fraction of above-canopy irradiance passing through the canopy below canopy irradiance](#) as a function of tree height (3.4 m) and density (275 trees ha⁻¹; Summers et al., 1997) via the equation of Parlane et al. (2006). This ~~irradiance~~ was then used in Beer's Law with a light-extinction coefficient of 0.5 (White et al., 2000) to determine LAI.

230 Diverse ecohydrological and isotope datasets were available at the BB [catchment](#) for model calibration (Table 2). Protocols used to collect and process these data are detailed in Kuppel et al. (2018a; 2018b). In most cases, model outputs were directly compared against relevant observed datasets. Simulated soil variables (~~VWC-volumetric water content~~ and bulk water isotopes) were exceptions; these are output for each soil layer and, therefore, do not directly correspond to depth-specific observations (c.f. Beven, 2006). To accommodate this, simulated ~~VWC-volumetric water content~~ timeseries for L1 and L2 were compared to observations made at the depth closest to the mid-point of each layer. Meanwhile, simulated soil water isotopes in L1 and L2 were compared with the ~~depth-average of observations made d isotopic composition of the soil within the soil~~ profile encompassed by each respective layer. Consequently, observations compared to simulated outputs from L1 and L2 could vary depending on soil depth parameterisation.

245 Model skill in simulating dynamics of ecohydrological and isotopic observations was quantified using the performance metrics in Table 2. Mean absolute error (~~MAE~~) was used for discharge to avoid over-emphasising of high flows ~~that can occur when using metrics based on mean squared errors~~ (Legates and McCabe, 1999; Krause et al., 2005). It was further used, and, for all isotope simulations given limited observational variability and daily timestep of the model (c.f. Gupta et al., 2009; Schaefeli

and Gupta, 2007). Root mean squared error (RMSE) was otherwise used as this is recommended if no information is available on error distributions (Chai and Draxler, 2004; Kuppel et al., 2018b). To determine behavioural parameter sets, model runs were first selected that simulated saturation areas <60% of total catchment area for at least 90% of the simulation period; this reflected mapping and modelling of the extent of saturation in the BB catchment (Birkel et al., 2010). Performance metrics for each calibration dataset were then ranked across all runs that satisfied this constraint. Runs were finally ordered by their worst-performing metric with the “best” 30 runs being retained as behavioural; this balanced the need to illustrate uncertainty in model outputs with the increased computational demand of producing spatial outputs required post-calibration.

Table 2: Datasets used in the calibration of ECH2O-iso and their temporal coverage (Full study period is 21.02.13 to 08.08.16).; The performance metrics used to quantify the skill of the model in simulating each dataset and the ranges of values achieved by the 30 behavioural model runs are also given.

Dataset	Temporal coverage	Metric ^a	Behavioural range
<u>Streamflow</u>	Full study period	MAE	0.026 to 0.033 m ³ s ⁻¹
<u>Soil moisture content</u>			
Forest A (10, 20 & 40 cm)	Full study period	RMSE	^b 0.10 to 0.27 m ³ m ⁻³
Forest B (10, 20 & 40 cm)	25 February 2015 onwards	RMSE	^b 0.11 to 0.19 m ³ m ⁻³
Gley (10, 30 & 50 cm)	Full study period	RMSE	^b 0.04 to 0.29 m ³ m ⁻³
Heather A (10, 20 & 40 cm)	Full study period	RMSE	^b 0.06 to 0.27 m ³ m ⁻³
Peat (10 cm)	Full study period	RMSE	0.02 to 0.10 m ³ m ⁻³
Peaty podzol (10, 30 & 50 cm)	Full study period	RMSE	^b 0.03 to 0.11 m ³ m ⁻³
<u>Green fluxes</u>			
Heather A: transpiration and evapotranspiration	31 July 2015 to 30 October 2015 &	RMSE	^c <u>Tr</u> : 0.50 to 0.69 mm d ⁻¹
	21 April 2016 to 03 August 2016		ET: 0.81 to 1.16 mm d ⁻¹
Heather B: transpiration and evapotranspiration	31 July 2015 to 30 October 2015 &	RMSE	^c <u>Tr</u> : 0.43 to 0.60 mm d ⁻¹
	31 March 2016 to 11 July 2016		ET: 0.78 to 0.95 mm d ⁻¹
Forest A: transpiration	08 July 2015 to 27 September 2015	RMSE	0.33 to 0.70 mm d ⁻¹
Forest B: transpiration	01 April 2016 onwards	RMSE	0.22 to 0.39 mm d ⁻¹

Formatted: Normal

Formatted: Font color: Auto

Formatted: Underline

Formatted: Font: Not Italic, Underline

Formatted: Font: Not Italic, Underline

Formatted: Superscript

<u>Net radiation</u>			
Bog weather station	10 October 2014 to 03 August 2016	RMSE	29 to 36 W m ⁻²
Hilltop weather station	22 April 2015 onwards	RMSE	40 to 58 W m ⁻²
Valley bottom weather station	10 October 2014 onwards	RMSE	29 to 39 W m ⁻²
<u>Streamflow: $\delta^2\text{H}$</u>			
	Full <u>study period</u>	MAE	2.7 to 8.2‰
<u>Soil $\delta^2\text{H}$ (2.5, 7.5, 12.5 and 17.5 cm)</u>			
Forest A: bulk soil water	29 September 2015 onwards (monthly)	MAE	^b 3.4 to 20.6‰
Forest B: bulk soil water	29 September 2015 onwards (monthly)	MAE	^b 3.8 to 7.5‰
Heather A: bulk soil water	29 September 2015 onwards (monthly)	MAE	^b 2.6 to 21.5‰
Heather B: bulk soil water	29 September 2015 onwards (monthly)	MAE	^b 4.2 to 8.2‰
<u>Groundwater $\delta^2\text{H}$</u>			
Deeper well 1 (Peat)	11 samples between 09 June 2015 and 22 July 2016	MAE	0.4 to 5.4‰
Deeper well 2 (Peat)	11 samples between 09 June 2015 and 22 July 2016	MAE	0.7 to 2.9‰
Deeper well 3 (Peaty gley)	11 samples between 09 June 2015 and 22 July 2016	MAE	0.7 to 6.7‰
Deeper well 4 (Peaty podzol)	11 samples between 09 June 2015 and 22 July 2016	MAE	0.7 to 3.4‰

Notes: ^aMAE = mean absolute error, RMSE = root mean squared error; ^bRange across first two soil layers of Ech_2O -iso; ^c $\text{Tr} = \text{transpiration}$, $\text{ET} = \text{evapotranspiration}$.

Formatted: Font: Not Italic, Underline

Formatted: Underline

Formatted: Font: Not Italic, Underline

Formatted: Font: Not Italic, Underline

Formatted: Underline

Formatted: Superscript

265 3.4 Regeneration scenarios

Extensive work characterising the structure of native pine stands at Abernethy Forest in the Cairngorms National Park (Parlane et al., 2006; Summers, 2018; Summers et al., 1997; 2008) was used to select two stages of forest regeneration for simulation. For context, [Supplementary Fig. S1](#) summarises the general sequence of natural pinewood regeneration. The thicket stage has the highest tree densities and near-complete canopy closure; consequently, this stage was selected because it will likely have ^sthe most substantial impact on water partitioning and catchment hydrology. Trees are ~40 years old whilst understorey development is limited. ~~The second chosen stage was a~~ Old open forest was chosen as the second stage and represents as a possible realisation of old-growth forest. This stage may be somewhat semi-natural with a canopy that is perhaps too open as a consequence -and, thus, characterised by a more open canopy than might be expected (reflect of past silvicultural practices and upland grazing (Summers et al., 2008). Consequently, regeneration of such a forest would require a rewilding trajectory

270

275 ~~that seeks to restore natural regeneration whilst also employing passive management to preserve characteristics of a landscape~~
~~that reflects elements of Scottish cultural heritage and/or the habitats provided by such a semi-natural environment~~
~~ing limited~~
~~modification by grazing pressures and selective felling; Summers et al., 2008). However, it was assumed to represent the near-~~
~~end point of a rewilding trajectory that balances human demands on the land with forest regeneration~~ (c.f. Deary and Warren,
2017). ~~Nonetheless, it was chosen as a possible, and a possible~~ “lowest impact” stage of late forest development ~~and, thus,~~
280 ~~offers an extreme contrast to the thicket scenario.~~ Trees are tall, old (~150 years) and sparsely distributed with an understorey
of well-developed shrubs.

The proportional coverage and characteristics of vegetation at each stage of forest regeneration are given in Table 1. Native
pinewoods, consisting of thicket/old open pine and a heather understorey, were assumed to fully regenerate on podzols and
285 rankers (Fig. 4h1c), reflecting the preference of pine for freely draining minerogenic soils (Mason et al., 2004). The available
regeneration area was limited in ranker cells containing scree or exposed bedrock such that the bare earth fraction remained
constant across scenarios, whilst regeneration did not occur on managed land at the catchment outlet or in pre-existing areas
of native pinewood on the northern hillslope (Fig. 4h1c). Bog woodland consisting of stunted bog pine, heather and *Molinia*
grass, was simulated to develop on the wetter peaty gleys (McHaffie et al., 2002; Steven and Carlisle, 1959; Summers et al.,
290 2008), whilst no regeneration was possible on the waterlogged peat (Fig. 4h1c). Spatial changes in vegetation cover for each
regeneration scenario relative to the baseline are shown in Fig. 2b-c. Scale factors relating calibrated values of *LAI* for pre-
existing pine to *LAI* of thicket, old open and bog pine were calculated as described in Sect. 3.3. For thicket/old open pine,
measured ~~fractions of below the above-~~canopy irradiance ~~passing through the canopy was were~~ available from Parlane et al.
(2006). ~~Estimates for bog pine and, hence, did not require estimation. For bog pine, irradiance was~~ again ~~obtained made~~
295 via the equation of Parlane et al. (2006). The heights of bog pine in each scenario were estimated by first calculating a “stunted”
growth rate (~0.06 m yr⁻¹) by dividing the height of present-day bog pine by an assumed age of 60 years. This was multiplied
by the age of pines in the thicket (40 years) and old open (150 years) forests to give bog pine heights of 2.4 m and 8.4 m for
each scenario, respectively. These values are broadly consistent with height measurements made by Summers et al. (2008) on
bog pine trees with an interquartile age range between 72 and 143 years.

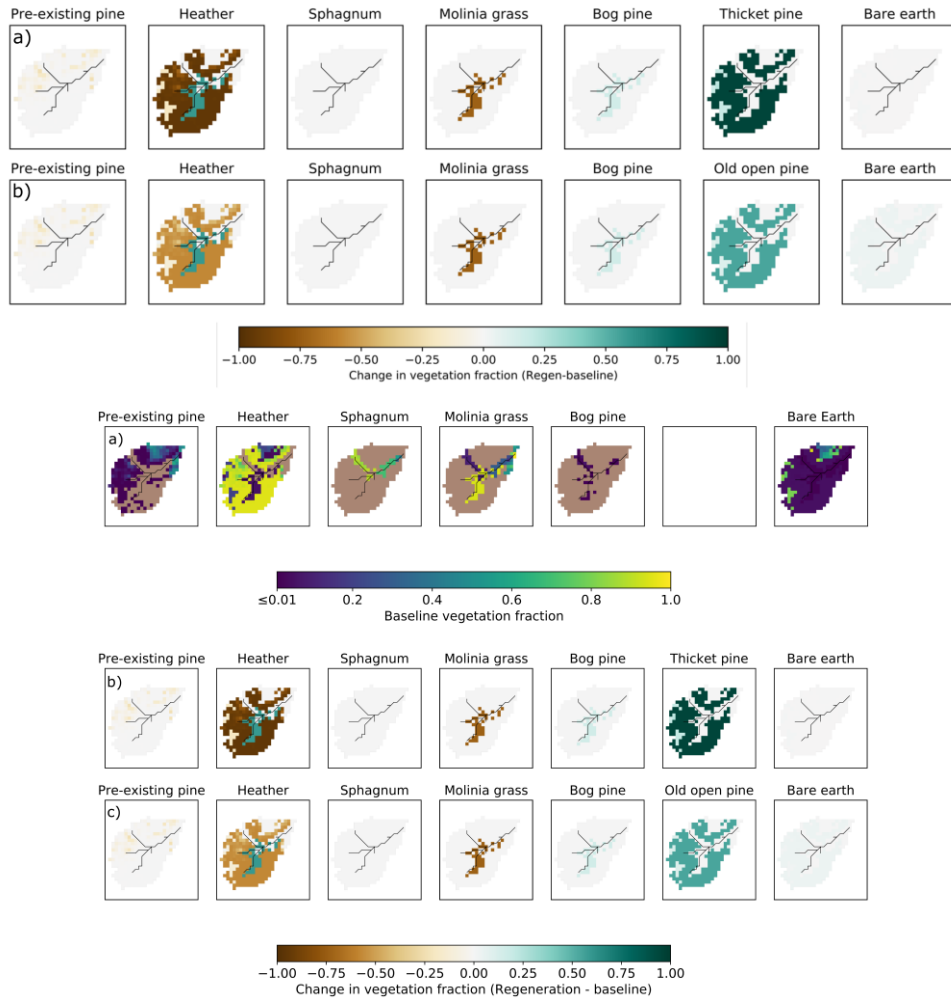


Figure 2: Maps showing a) Proportional vegetation coverage in the present-day baseline scenario, and b) Changes in vegetation cover for the a) Thicket scenario and b) Old open forest scenario. Changes are reported as regeneration scenario minus baseline scenario. In a), coverages of zero are signified by brown cells.

305

310 Simulations were driven by the 30 behavioural parameter sets obtained from the baseline calibration and undertaken for the same time period (21 February 2013 to 08 August 2016) with 30 years of spin-up. As previously stated, soil properties remained unchanged in the regeneration scenarios. Additionally, the vertical root distribution parameter was consistent amongst pine vegetation types as after the sapling stage, the most significant changes to Scots pine rooting characteristics are expressed in the horizontal rather than vertical direction (Laitakari, 1927; Makkonen and Helmisaari, 2001). Potential effects of such changes on the vertical root distribution would likely already be captured by the sampling range of this parameter for pre-existing pine (Table S2).

315 3.5 Change analysis

To contextualise changes to water flux partitioning, simulated maximum root zone (~~RZ~~) and interception storage capacities were quantified for each scenario. For each vegetation type in a given grid cell, ~~root zone~~RZ storage capacity was defined as the sum of maximum plant available ~~VWC-volumetric water content~~ in each layer weighted by root fraction, multiplied by the coverage-weighted average rooting depth of all vegetation types in the cell. A coverage-weighted sum across all present 320 vegetation types then yielded the total ~~RZ-root zone~~ storage capacity for the cell. The total interception storage capacity of each cell was similarly calculated, with the interception storage capacity of each vegetation type obtained by multiplying the parameters *LAI* and *maximum canopy storage* (Table S2). Average values of ~~RZ-root zone~~ and interception storage capacity for the catchment were then calculated.

325 Catchment-scale flux partitioning was assessed by quantifying seasonally averaged totals of simulated discharge at the outlet, and catchment-averaged GW recharge, soil and interception evaporation, and transpiration fluxes. Seasons were defined as April to September (“Active season”) and October to March (“Dormant season”), broadly corresponding to ~~biologically active and dormant~~ periods ~~of biological growth and dormancy in north-east Scotland~~, respectively (Dawson et al., 2008). Seasonal 330 ~~volume-weighted~~ly averaged water ages were also calculated for selected stores and fluxes. Daily timeseries of discharge, stream isotopic composition and water age provided a spatially integrated insight into how regeneration affected modelled catchment hydrology at a higher temporal resolution. To better understand spatial drivers of changes to catchment-scale flux partitioning, differences in seasonal daily average “blue” and “green” fluxes between each scenario and the baseline were spatially disaggregated.

335 To assess how regeneration impacts hydrological source areas and runoff generation, the spatial extent of hydrological connectivity was quantified under contrasting flow conditions. A cell was considered hydrologically connected if overland flow (OLF) was simulated for the cell and all downslope cells along the flow path to the stream. ~~No minimum threshold of OLF was imposed for a cell to be considered connected (c.f. Turnbull and Wainwright, 2019) as EcH₂O-iso simulates re-~~ 340 ~~infiltration along a given flow path which can prevent upslope cells producing OLF from connecting to the stream (Maneta~~

and Silverman, 2013). Flow path lengths for connected cells were calculated by accumulating the straight line or diagonal lengths (dependent on local flow direction) of all cells along the flow path (c.f. Turnbull and Wainwright, 2019). Four different flow conditions were considered for the connectivity analysis with each assessed using OLF simulations from a representative date: 1) Summer baseflows (22.07.2013), 2) Small to moderate events during summer and autumn/winter rewetting (15.09.2014), 3) Larger summer events (20.07.2016), and 4) Large winter events (30.12.2015). A threshold of OLF was not implemented as water can infiltrate along a flow path in EcH₂O-iso (Maneta and Silverman, 2013). Three dates were selected for connectivity analysis. The first, 22 July 2013, was during a particularly dry early summer. The second, 10 August 2014, was during a moderately wet late summer period caused by a frontal storm. The third, 30 December 2015, was at the height of some of the worst flooding seen for 100 years in NE Scotland caused by Storm Frank (Marsh et al., 2016).

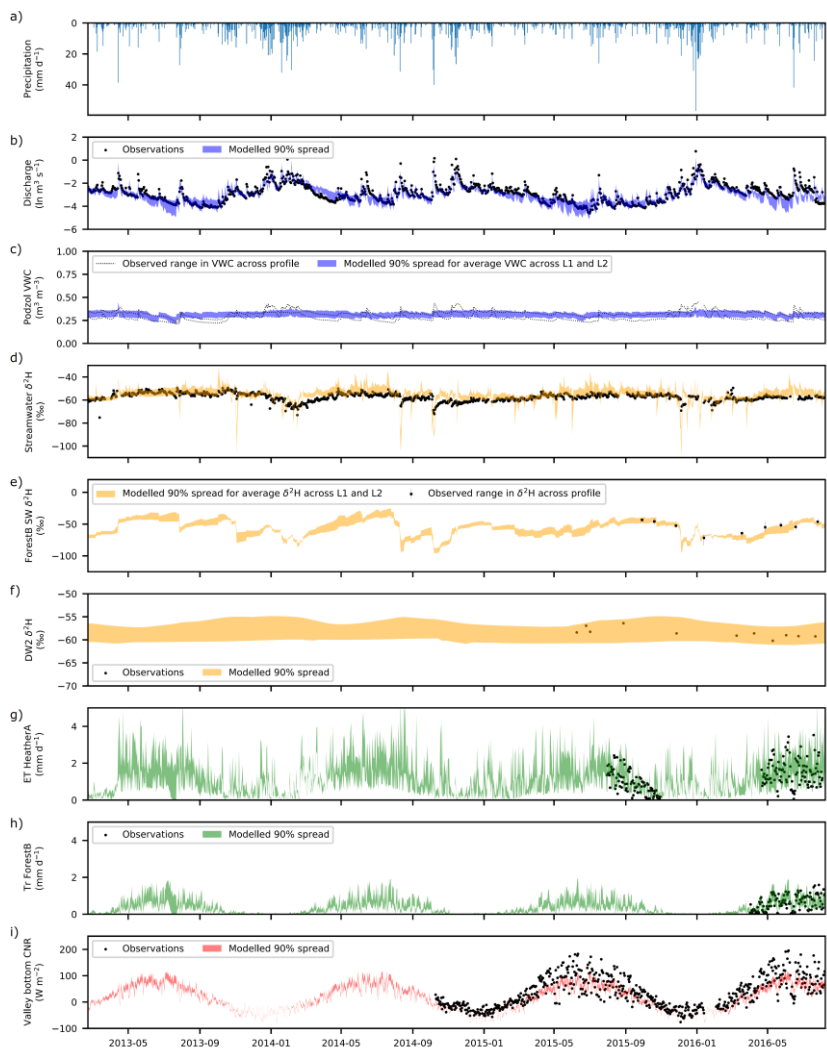
350 4 Results

4.1 Baseline calibration

Figure 3 summarises the skill of the model in simulating “blue” and “green” fluxes, isotope dynamics, and net radiation at selected monitoring locations (remaining simulations shown in Figs. S2-5). Performance metrics and calibrated parameter ranges and performance metrics are given in Tables S2 and S2, respectively. Stream discharge was generally well simulated, with only occasional under-prediction of baseflows (e.g. summer 2016) and the most extreme events (Fig. 3b). At most sites, modelled VWC-volumetric water content in L1 and L2 was bracketed by the range observed across the soil profile (Figs. 3e and S2), although simulations were sometimes less dynamic than observations and RMSEs-root mean squared errors could be large (Table 2). However, this likely reflects the commensurability issues highlighted in Sect. 3.3 (also relevant for soil water isotopes), and the fact that Heather Site A and Forest Site A fell within the same model cell. The model was generally successful in reproducing dynamics of streamwater, soil water and groundwater isotopes (Table 2; Figs. 3d-f and S3), implying internal catchment functioning was reasonably well-captured. Stream isotopes were sometimes over-enriched, suggesting slightly high soil evaporation (Fig. 3d); however, the variability was generally well-captured. Larger deviations during events likely reflect structural limitations of the model (e.g. the ability of OLF to traverse the catchment within one timestep). Excessive evaporation was not apparent from simulated soil water isotopes (Figs. 3e and S3), although averaging over L1 and L2 could obscure the effects of evaporative fractionation in the former. The model had skill in simulating ET and forest transpiration (Table 2; Figs. 3g-h and S4). However, underestimation of heather transpiration for the heather (Fig. S4) may indicate too much excessive radiative energy being used for evaporation. Seasonality in net radiation was well simulated though; however, the magnitude of shorter-term variability was under-estimated in summer (Table 2; Figs. 3i and S5).

370 **4.2 Impact of regeneration on water storage capacity**

Figure 4 summarises simulated RZ-root zone and interception storage capacities for each scenario. Median RZ-root zone storage capacity increased by 21 mm in the thicket forest scenario (Fig. 4a) reflecting replacement of heather by thicket pine (Fig. 2a2b) with deeper roots (Table S2) that increase access to water stored in L2 and L3. Small increases in RZ-root zone storage capacity were simulated for the old open forest scenario, albeit with greater overlap with the baseline (Fig. 4a), likely reflecting the more balanced composition between pine and heather (Fig. 2b2c). This, along with greater proportional coverage of bare earth (Fig. 2bc), may also explain overlap of interception storage capacity between the old open forest and baseline scenarios (Fig. 4b). The greater coverage of thicket pine (Fig. 2ba) with a dense canopy substantially increased interception storage capacity for the thicket forest scenario (Fig. 4b).



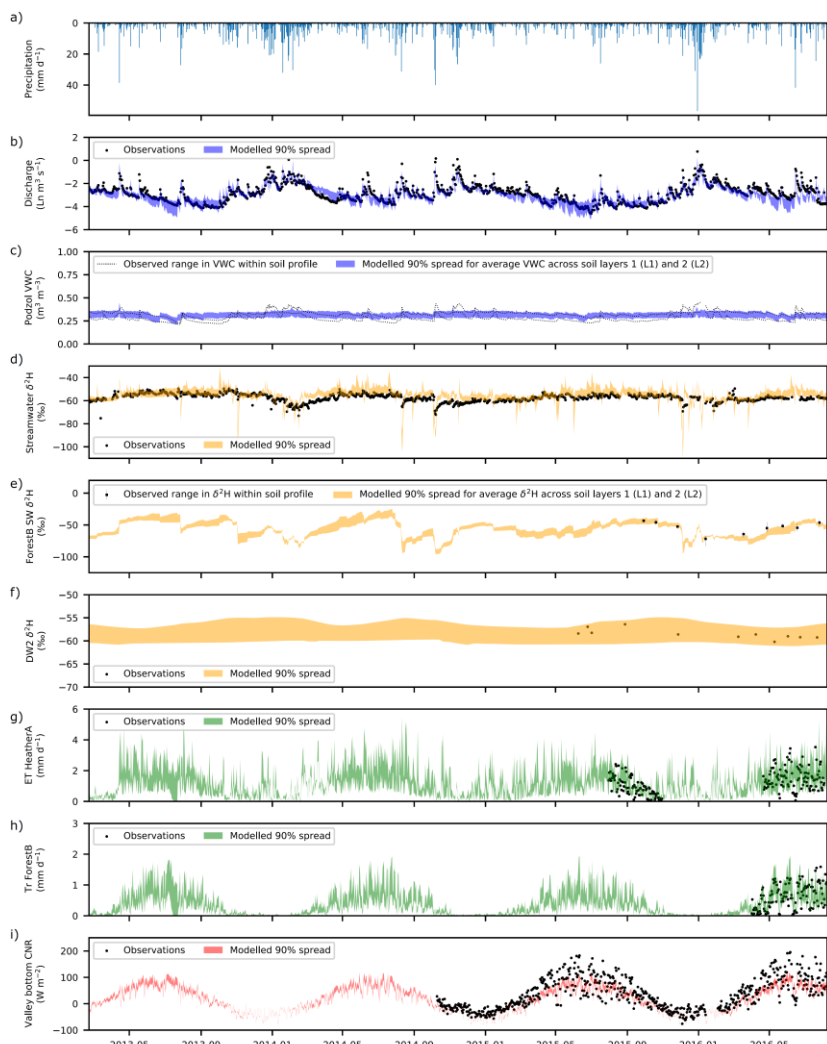


Figure 3: Time series of a) Precipitation; and of observed and simulated b) Natural logarithm (Ln) of stream discharge; c) Volumetric water content (VWC) at the peaty podzol site; d) Stream $\delta^2\text{H}$ composition; e) Bulk soil water (SW) $\delta^2\text{H}$ under Forest B; f) Groundwater $\delta^2\text{H}$ at Deeper Well 2 (DW2); g) Total evapotranspiration (ET) for Heather A; h) Transpiration (Tr) for Forest B; i) Net radiation (CNR) at the valley bottom weather station. 90% spread of simulations are from the 30 behavioural model runs.

380

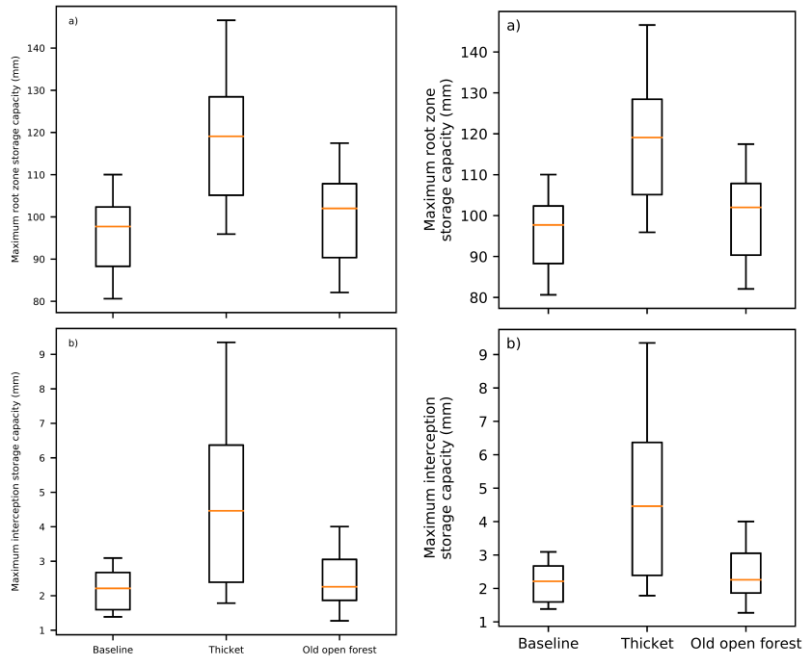
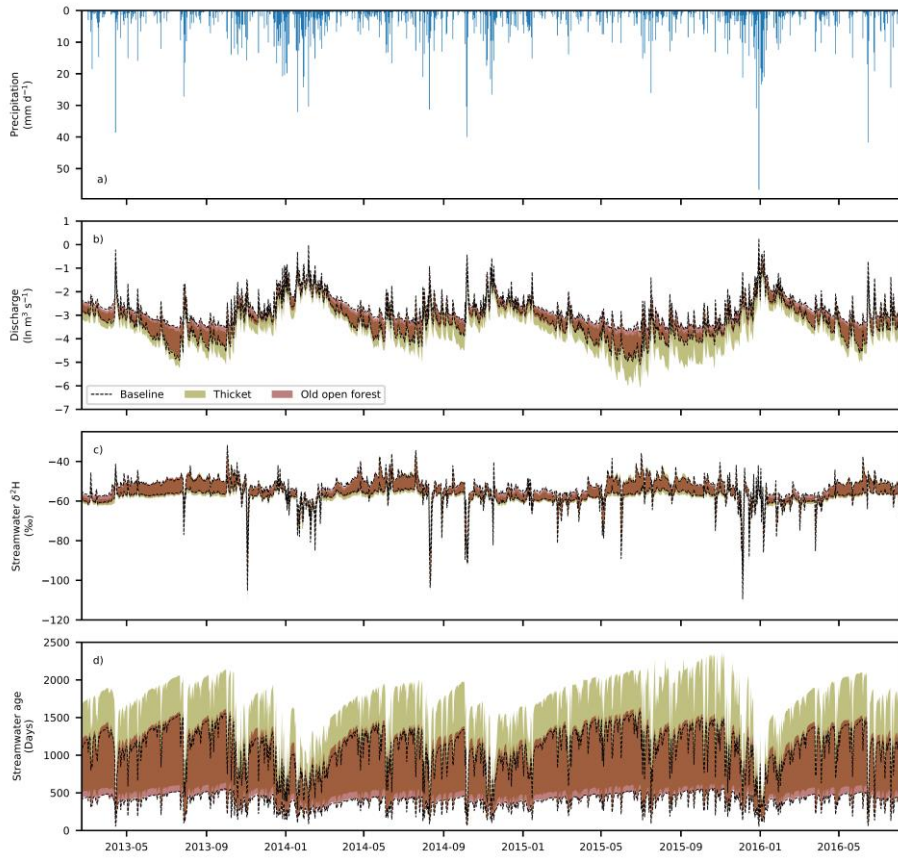


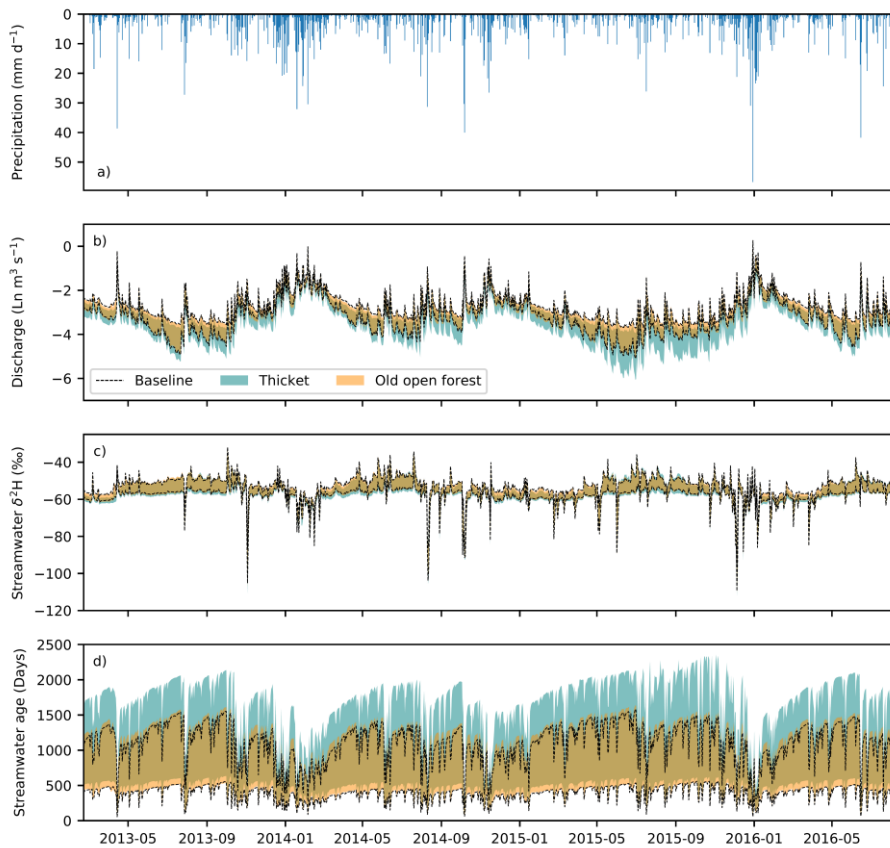
Figure 4: Boxplots showing maximum a) Root zone storage capacity and b) Interception storage capacity, for the baseline and forest regeneration scenarios. The median is shown by the orange line whilst the box extends from the lower to upper quartiles. The 5th and 95th percentiles are given by the tails.

4.3 Changes to catchment-scale water flux partitioning

Figure 5 shows how impacts of modelled regeneration integrated to affect the simulated quantity and isotopic composition of streamflow. The greatest differences in discharge was most notably reduced between the in the thicket and baseline scenarios. Proportional reductions in discharge (as revealed by considering its natural logarithm) appeared to show an annual cycle, generally increasing in magnitude through the summer months and into the autumn/winter rewetting period before being “reset” by a sufficiently large winter event that resulted in more limited divergence of subsequent winter and spring flows. Consequently, low to moderate flows during the summer and autumn/winter rewetting period were most affected in the thicket scenario whilst higher flows remained relatively consistent. were for moderate to low flow periods with the magnitudes of

~~high flows being relatively consistent (Fig. 5b).~~ For the old open forest scenario, discharge was similar to the baseline. For both regeneration scenarios, simulated stream isotope dynamics were comparable to the baseline ~~(Fig. 5e)~~; however, streamwater could sometimes be slightly more depleted in summer for the thicket scenario indicating reduced soil evaporation.





405 **Figure 5:** Timeseries of a) Observed precipitation, and simulated b) Natural logarithm (Ln) of stream discharge; c) Streamwater $\delta^2\text{H}$ composition; d) Streamwater age. In b) to d), the area between the two black lines represents the 90% spread of behavioural simulations for the baseline scenario whilst the shaded areas show the same for the thicket and old open forest scenarios. Areas of darker gold-coloured shading occur where simulations for the two regeneration scenarios overlap, and the areas that are shaded represent the 90% spread of simulations from the 30 behavioural model runs.

410

Table 3 summarises the changes to seasonally averaged water flux totals. Overall, behavioural models consistently simulated a decrease in seasonally averaged discharge for the thicket scenario (Table 3a-b). This resulted from increased interception evaporation (Table 3e-f) and transpiration (Table 3i-j), and decreased GW recharge (Table 3e-d). Recharge was most reduced

for the dormant season Oct-Mar, concurrent with the greatest increase in interception evaporation. Soil evaporation was lower for the thicket scenario (Table 3g-h), likely reflecting limits imposed by lower soil moisture due to greater interception evaporation and transpiration losses, and reduced penetration of radiation through the thicket canopy. Differences in seasonally averaged fluxes were much smaller between the old open forest and baseline (Table 3b, d, f, h, j), resulting in the median and 5th/95th percentile seasonally averaged flux totals generally being similar for the two scenarios (Table 3a, c, e, g, i). However, there was a repartitioning of water between increased interception evaporation and reduced GW recharge for the dormant season Oct-Mar that contributed to a ~30 mm decrease in simulated median total discharge (Table 3a).

Table 3: Seasonally averaged water flux totals and differences in seasonally averaged totals between the regeneration and baseline scenarios. Totals and differences were calculated for each behavioural run individually and summarised by the median and 5th/95th percentile (in square brackets) values across all behavioural runs. Differences are reported as regeneration scenario minus baseline and help indicate whether the simulated direction of change in each flux was consistent amongst behavioural models. Active and dormant seasons cover April to September and October to March, respectively.

	<u>Median [5th/95th percentile] seasonally averaged flux totals (mm over summary period)</u>		<u>Median [5th/95th percentile] differences in seasonally averaged flux totals (mm over summary period)</u>	
	<u>Active</u>	<u>Dormant</u>	<u>Active</u>	<u>Dormant</u>
<u>Outlet stream discharge</u>				
<u>Baseline</u>	196 [159, 232]	449 [415, 481]	=	=
<u>Thicket</u>	143 [97, 202]	316 [258, 435]	-64 [-97, -8]	-129 [-178, -26]
<u>Old open forest</u>	190 [159, 230]	416 [369, 486]	-12 [-31, 18]	-29 [-59, 15]
<u>Groundwater recharge</u>				
<u>Baseline</u>	161 [140, 190]	353 [283, 402]	=	=
<u>Thicket</u>	107 [68, 156]	277 [224, 349]	-63 [-93, -5]	-80 [-109, -15]
<u>Old open forest</u>	153 [129, 185]	336 [269, 382]	-9 [-27, 19]	-18 [-37, 6]
<u>Interception evaporation</u>				
<u>Baseline</u>	102 [81, 131]	77 [62, 90]	=	=
<u>Thicket</u>	182 [104, 234]	196 [102, 253]	83 [-3, 124]	118 [27, 168]

<u>Old open forest</u>	<u>116 [74, 159]</u>	<u>106 [61, 150]</u>	<u>19 [-24, 43]</u>	<u>31 [-10, 64]</u>
<u>Soil evaporation</u>				
<u>Baseline</u>	<u>74 [52, 94]</u>	<u>41 [35, 45]</u>	<u>-</u>	<u>-</u>
<u>Thicket</u>	<u>44 [34, 57]</u>	<u>28 [22, 34]</u>	<u>-32 [-47, -8]</u>	<u>-12 [-17, -7]</u>
<u>Old open forest</u>	<u>72 [55, 91]</u>	<u>37 [32, 41]</u>	<u>-2 [-12, 13]</u>	<u>-4 [-6, 0]</u>
<u>Transpiration</u>				
<u>Baseline</u>	<u>66 [52, 80]</u>	<u>6 [4, 8]</u>	<u>-</u>	<u>-</u>
<u>Thicket</u>	<u>89 [71, 121]</u>	<u>12 [9, 20]</u>	<u>27 [11, 47]</u>	<u>6 [3, 13]</u>
<u>Old open forest</u>	<u>58 [45, 76]</u>	<u>6 [5, 8]</u>	<u>-7 [-14, 3]</u>	<u>0 [-1, 2]</u>

	Median [5th/95th-percentile]-seasonally averaged flux-totals (mm over summary-period)		Median [5th/95th-percentile]-differences in seasonally-averaged flux-totals (mm over summary-period)	
	Apr to Sep	Oct to Mar	Apr to Sep	Oct to Mar
<i>Outlet stream discharge</i>	a)		b)	
<u>Baseline</u>	<u>495.9 [158.8, 231.6]</u>	<u>449.2 [414.7, 480.5]</u>	<u>-</u>	<u>-</u>
<u>Thicket</u>	<u>443.3 [97.2, 201.7]</u>	<u>316.0 [258.4, 434.6]</u>	<u>-63.8 [-97.3, -7.8]</u>	<u>-128.7 [-178.0, -26.4]</u>
<u>Old open forest</u>	<u>489.5 [158.6, 229.6]</u>	<u>416.2 [369.1, 486.4]</u>	<u>-12.0 [-31.1, 18.0]</u>	<u>-28.7 [-59.3, 15.0]</u>
<i>GW Recharge</i>	e)		d)	
<u>Baseline</u>	<u>461.3 [140.0, 190.1]</u>	<u>352.7 [282.9, 402.0]</u>	<u>-</u>	<u>-</u>
<u>Thicket</u>	<u>407.0 [68.1, 156.1]</u>	<u>277.0 [223.7, 348.7]</u>	<u>-62.6 [-92.7, -5.5]</u>	<u>-80.2 [-109.0, -15.4]</u>
<u>Old open forest</u>	<u>453.0 [128.5, 185.2]</u>	<u>335.9 [269.4, 381.5]</u>	<u>-9.3 [-26.7, 19.1]</u>	<u>-17.6 [-36.5, 6.5]</u>
<i>Interception evaporation</i>	e)		f)	
<u>Baseline</u>	<u>402.2 [80.8, 131.4]</u>	<u>76.9 [61.6, 90.2]</u>	<u>-</u>	<u>-</u>

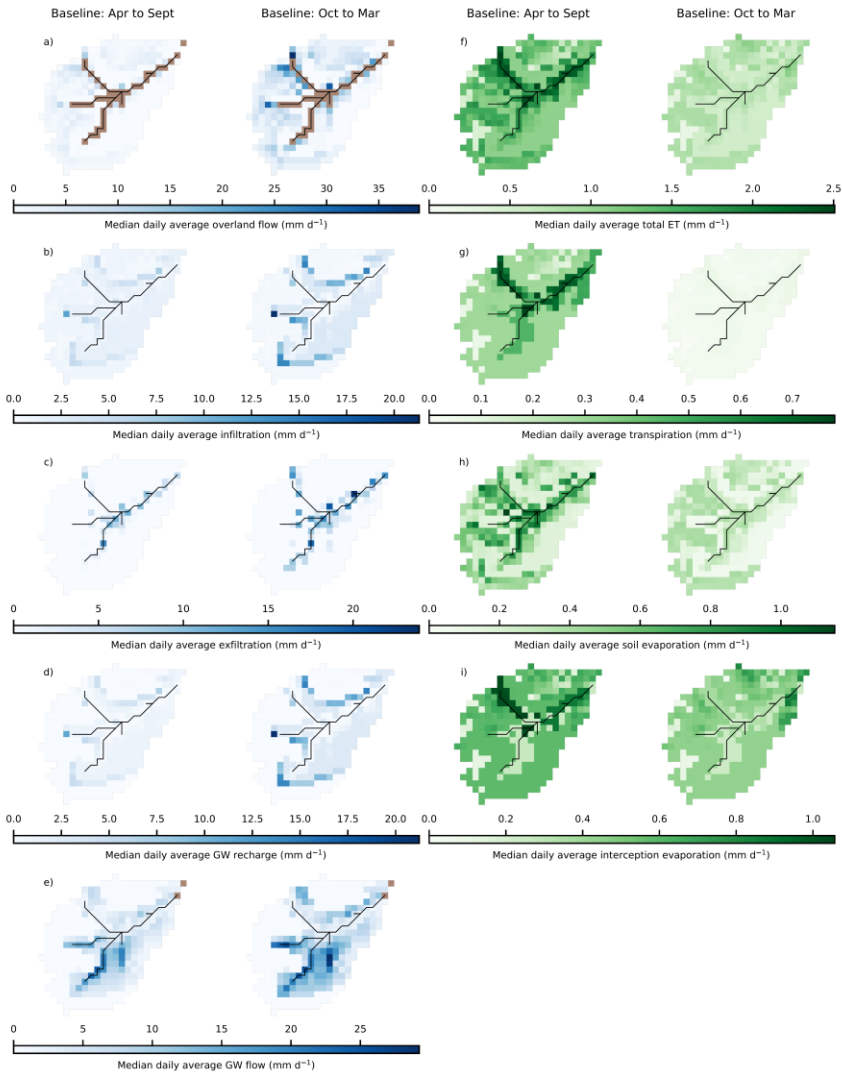
Thicket	182.5 [103.8, 234.2]	196.3 [102.2, 253.0]	82.6 [-3.0, 123.6]	118.5 [26.7, 167.6]
Old open forest	115.8 [73.8, 158.9]	105.6 [60.9, 150.0]	19.4 [-24.4, 42.6]	31.3 [-9.8, 64.3]
<i>Soil evaporation</i>		g)	h)	
Baseline	74.2 [52.3, 93.5]	41.2 [35.0, 44.6]	-	-
Thicket	44.0 [34.0, 57.1]	28.2 [22.1, 33.6]	-32.3 [-47.3, -7.6]	-12.4 [-16.9, -6.9]
Old open forest	72.0 [55.5, 90.5]	37.5 [32.5, 40.8]	-1.7 [-12.4, 13.0]	-3.7 [-5.9, 0.1]
<i>Transpiration</i>		i)	j)	
Baseline	66.4 [51.7, 79.9]	6.1 [4.3, 7.7]	-	-
Thicket	89.4 [71.5, 120.7]	12.1 [8.6, 19.8]	27.1 [11.2, 47.4]	6.1 [2.8, 12.8]
Old open forest	57.6 [45.4, 75.5]	6.1 [4.6, 8.4]	-6.8 [-13.7, 2.9]	0.0 [-1.0, 1.7]

4.4 Spatio-temporal dynamics of baseline flux partitioning

430 Figure 6 summarises spatial dynamics of median seasonal daily average “blue” and “green” fluxes for the baseline scenario. Simulated OLF was more limited for [the active season Apr–Sept \(Fig. 6a\)](#). The largest fluxes were simulated for the peats and peaty gleys, with some OLF also being generated by the ranker soils on the hillslopes. The latter is interpreted as representing the rapid near-surface flows in the shallow rankers that are driven by emergence of bedrock fracture flow at slope breaks. OLF fluxes were greater and had similar spatial patterns for [the dormant season Oct–Mar](#) with additional fluxes generated from the podzols on lower hillslopes in the north and south ([Fig. 6a](#)). Vertical movement of water (infiltration and GW recharge) was greatest in winter and mostly occurred on the podzols; the largest fluxes were simulated at the boundaries between the podzols and rankers ([Fig. 6b and d](#)) reflecting lateral flows from upslope moving vertically in deeper soils. Water was then simulated to move downslope as GW ([Fig. 6e](#)) to sustain saturation in the valley bottom, as evidenced by high exfiltration fluxes especially in [the dormant season Oct–Mar \(Fig. 6e\)](#).

440 Daily average fluxes of ET were simulated as greatest for [the active season Apr–Sept](#), particularly in the valley bottom (Fig. 6f). This was facilitated by the wet peat and peaty gleys maintaining transpiration ([Fig. 6g](#)) and soil evaporation ([Fig. 6h](#)), and further by evaporation of water intercepted by the *Sphagnum* “canopy” ([Fig. 6i and Table S2](#)). Dominance of vertical sub-surface fluxes ([Fig. 6b and d](#)) limited transpiration ([Fig. 6g](#)) and, particularly, soil evaporation ([Fig. 6h](#)) from the podzols, reducing total ET fluxes ([Fig. 6f](#)). For [the dormant season Oct–Mar](#), spatial patterns in total ET were less distinct ([Fig. 6f](#)) reflecting reduced soil and interception evaporation in the valley bottom ([Fig. 6h–i](#)) and the fact that daily transpiration fluxes

were essentially ~~0-zero~~(Fig. 6g). A notable pattern was that total ET was ~~particularly greatest-elevated~~ where there was substantial pre-existing pine (Figs. 4-2a and 6f) due to sustained interception evaporation (~~Fig. 6i~~).



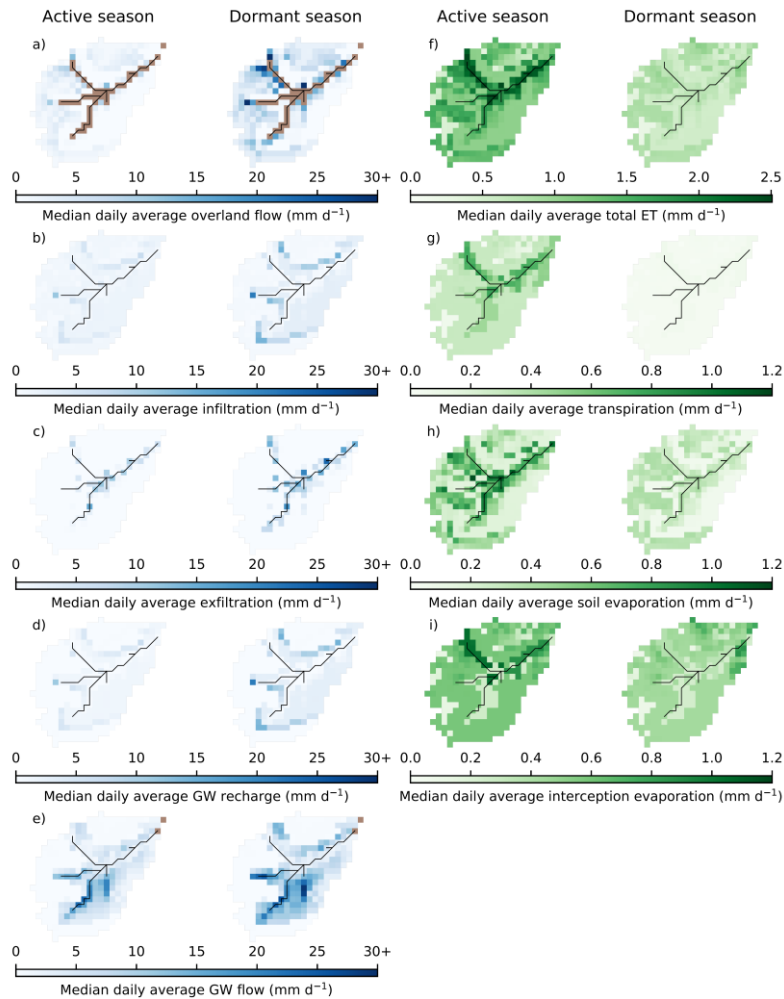


Figure 6: Maps showing median daily average fluxes of the baseline scenario for the active in-(April to September) and dormant (October to March) seasons for: a) Cell-to-cell Overland flow; b) Infiltration into L1-the first soil layer (L1) of the soil; c) Exfiltration to the surface; d) Groundwater (GW) recharge; e) Groundwater-Cell-to-cell lateral GW flow; f) Total evapotranspiration (ET); g) Transpiration; h) Soil evaporation; and i) Interception evaporation. Brown cells in a) and e) are channel and outlet cells for which ECH₂O-iso does not simulate cell-to-cell overland and lateral GW flows. Colourbar for "blue" fluxes is truncated at upper limit to

455

Formatted: Subscript

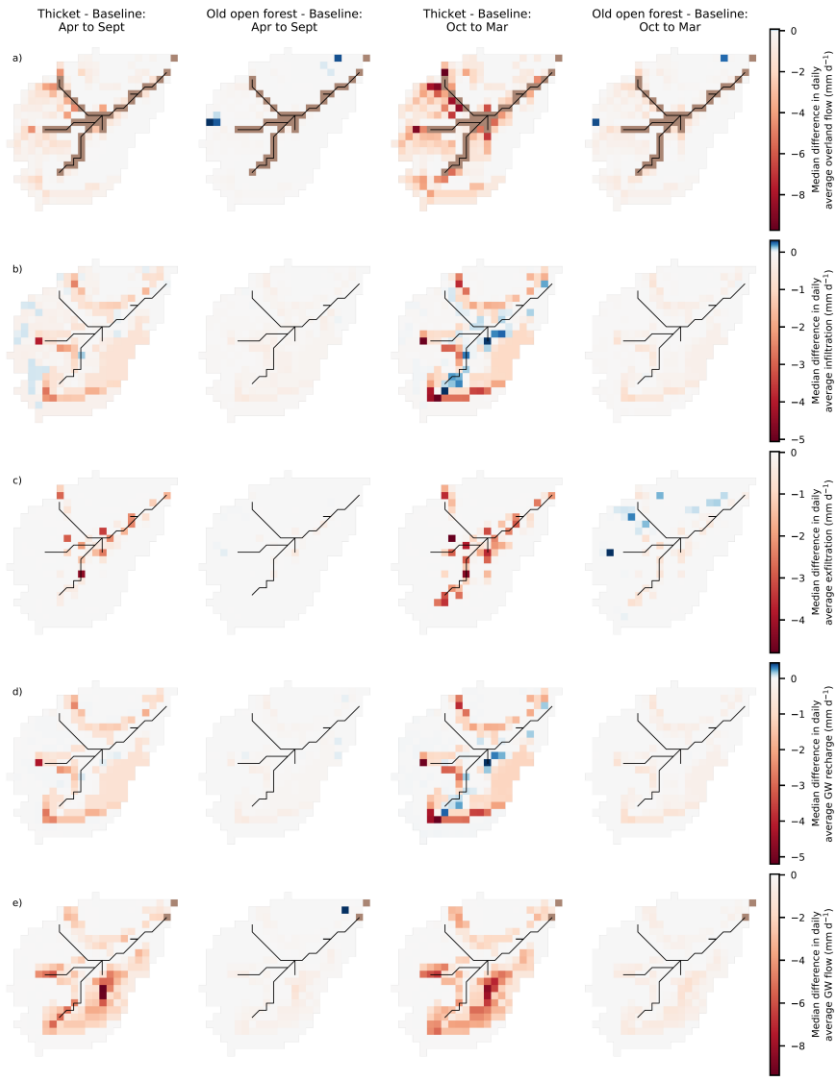
aid presentation of spatial patterns (largest flux is 38.9 mm d⁻¹ for overland flow). Note that total ET is on a different scale to the other “green” fluxes.

4.5 Spatio-temporal disaggregation of regeneration effects on flux partitioning

Median differences in seasonal daily average “blue” fluxes were most dramatic for the thicket scenario (Fig. 7). For both the active and dormant seasons Apr-Sept and Oct-Mar, similar spatial patterns were simulated, although differences tended to be greater for the latter. More limited OLF generation by the rankers (Fig. 7a) led to similar-magnitude reductions in daily average infiltration and GW recharge on the podzols (Fig. 7b and d). Consequently, downslope movement of GW also decreased in both seasons Apr-Sept and Oct-Mar (Fig. 7e). This contributed to a drying out of the valley bottom (especially in the dormant season Oct-Mar) even though local regeneration was limited (Fig. 2ba). Daily average OLF fluxes were simulated to decrease around the fringes of the stream for both seasons Apr-Sept and Oct-Mar (Fig. 7a). The largest decreases occurred in the NW north-west of the catchment as a direct consequence of reduced OLF from upslope. Elsewhere, OLF reductions strongly reflected the reductions in upslope GW subsidies as evidenced by consistently decreased exfiltration fluxes (Fig. 7c) and increased infiltration of incoming precipitation in the valley bottom for the dormant season Oct-Mar (Fig. 7b) to replenish drier soil and GW stores (Fig. 7d).

Similar spatial dynamics were simulated for the old open forest scenario, however median differences in seasonal daily average fluxes were much reduced (Fig. 7). It is also noteworthy that even in the dormant season Oct-Mar, the valley bottom dried out less than in the thicket scenario; daily average GW flows through the podzols were only simulated to decrease by $<1.5 \text{ mm d}^{-1}$ (Fig. 7e), whilst no increases in infiltration or GW recharge were simulated in the valley bottom (Fig. 7b and d).

Differences in seasonal daily average “green” fluxes were also more apparent in the thicket scenario (Fig. 8). Daily average ET from the podzols and rankers was simulated to increase throughout the year (Fig. 8a). For the active season Apr-Sept, this resulted from greater transpiration (Fig. 8b) and, predominantly, interception evaporation (Fig. 8d), reflecting the increased coverage of thicket pine (Fig. 2ba). Reduced penetration of radiative energy through the thicket canopy, and limits imposed by greater water losses to transpiration and interception evaporation, decreased simulated daily average soil evaporation (Fig. 8e). For the dormant season Oct-Mar, increased ET was more driven by greater interception evaporation (Fig. 8d). ET from the bog woodland was similar to the baseline (Fig. 8a). This was due to decreased transpiration from reduced cover of potentially deep-rooted (Aerts et al., 1992; Taylor et al., 2001) *Molinia* grass (Figs. 2ab and 6b) being compensated by increases in soil (Fig. 8e) and, particularly, interception evaporation (Fig. 8d). Daily average ET for the active season Apr-Sept decreased in some areas of peat in the NW of the catchment, despite no regeneration having taken place (Fig. 8a). This would be consistent with drying of the valley bottom limiting summer transpiration (Fig. 8b). Given small transpiration demands in Oct-Nov (Fig. 6g) no reduction in ET was simulated.



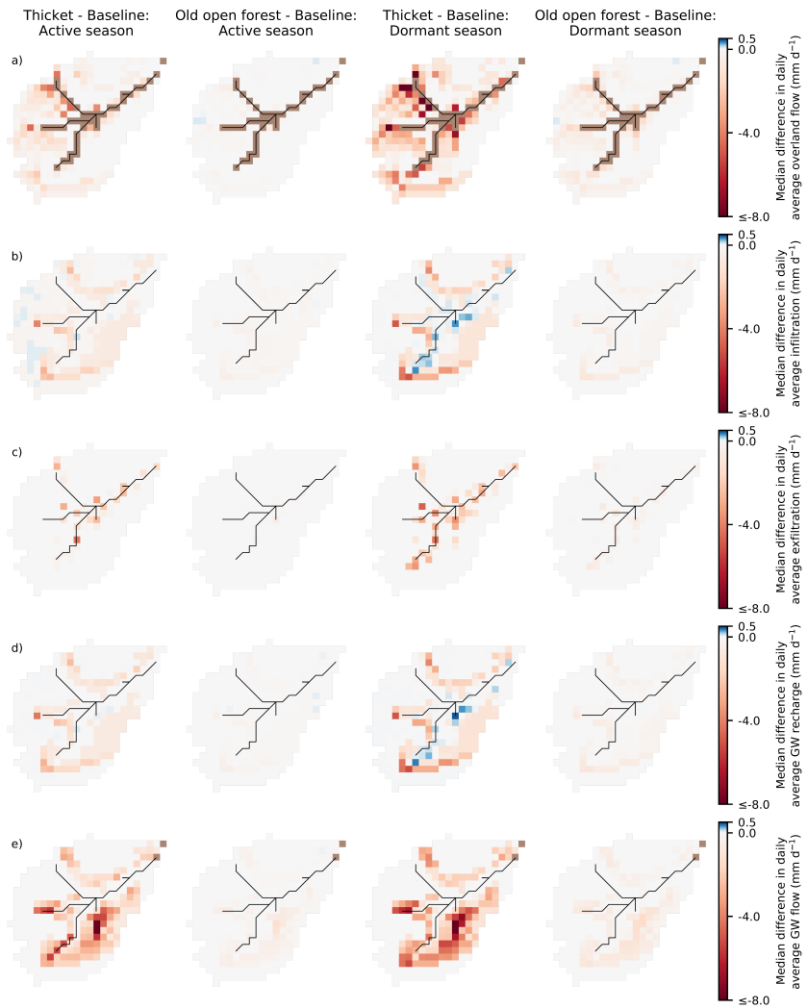
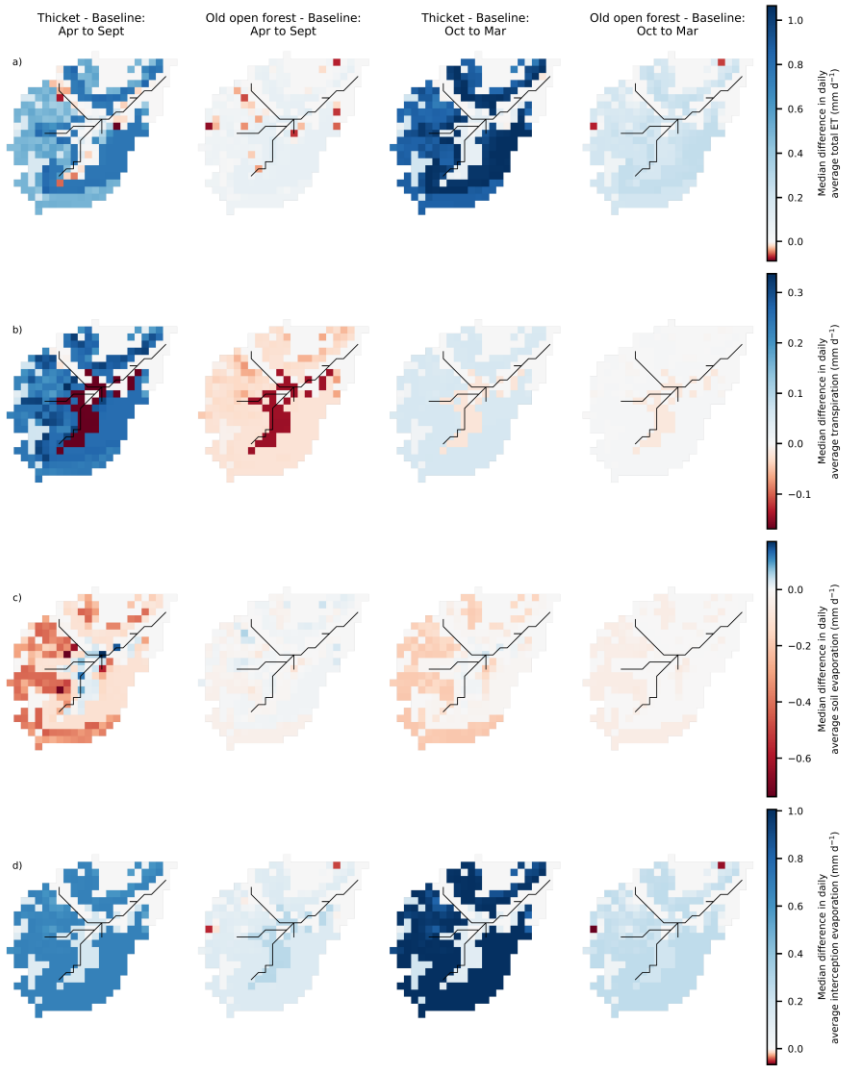


Figure 7: Maps showing the median difference in daily average “blue” fluxes for the active (April to September) - and dormant (October to March) seasons: a) Cell-to-cell overland flow; b) Infiltration into the first soil layer (L1) of the soil; c) Exfiltration to the surface; d) Groundwater (GW) recharge; e) Cell-to-cell lateral GW flow. Differences are reported as regeneration scenario minus baseline scenario. Brown cells in a) and e) are channel and outlet cells for which ECH₂O-iso does not simulate cell-to-cell overland and lateral GW flows. Colourbar is truncated at lower limit to aid presentation of spatial patterns (largest negative difference is -9.7 mm d⁻¹ for overland flow).

495

500



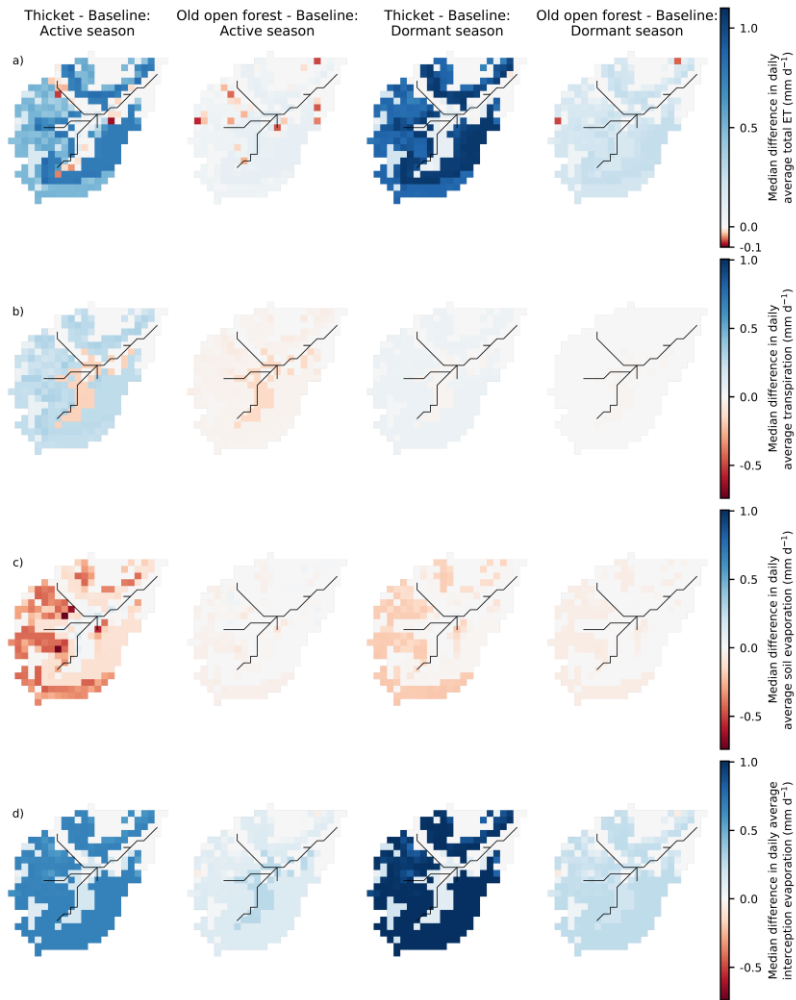


Figure 8: Maps showing the median difference in daily average “green” fluxes for the active (April to September) and dormant (October to March) seasons: a) Total evapotranspiration (ET); b) Transpiration; c) Soil evaporation; and d) Interception evaporation. Differences are reported as regeneration scenario minus baseline scenario. Note that total ET is on a different scale to the other fluxes.

505

Differences in simulated ET were much more subdued for the old open forest scenario (Fig. 8a). For the active season Apr–Sept, soil evaporation on the rankers and podzols, in particular, and rankers remained similar to the baseline, (Fig. 8c) whilst transpiration showed a more consistent slight decrease (Fig. 8b), likely reflecting greater bare earth coverage (Fig. 2b). This offset greater losses to interception evaporation (Fig. 8d) so that only very-small increases in total ET were simulated. Very Ssmall ET decreases mostly reflected replacement of larger clusters of pre-existing pine with old open forest (Fig. 2c) reducing transpiration (Fig. 8b). A larger increase in interception evaporation from the old open forest (Fig. 8d) drove the increases in ET from the podzols and rankers for the dormant season Oct–Mar (Fig. 8a).

4.6 Effects of regeneration on ages of “blue” and “green” water fluxes

Streamflow, lateral GW outflows and soil water/evaporation were near-consistently simulated to have older average ages in the thicket scenario relative to the baseline (Table 4); however, change magnitudes were often less than the width of simulation uncertainty bounds leading to overlap in flux ages. Simulated daily dynamics revealed that streamwater ages for the thicket scenario could be much older for low to moderate flows, although uncertainty bounds were again wide (Fig. 5d). Relatively young streamwater ages persisted in larger events. Transpiration fluxes were the only ones to indicate a possible slight preference for younger water through a reduction in 95th percentile average ages (Table 4i–j). For old open forest, age characteristics were generally restored to those simulated for the baseline (Table 4).

Table 4: Seasonally averaged water flux ages and differences in seasonally averaged ages. Averages and differences were calculated for each behavioural run individually and summarised by the median and 5th/95th percentile (in square brackets) values across all behavioural runs. Differences are reported as regeneration scenario minus baseline and help indicate whether the simulated direction of change in the average age of each flux was consistent amongst behavioural models. Active and dormant seasons cover April to September and October to March, respectively.

	Median [5 th /95 th percentile] seasonally averaged water age (days)		Median [5 th /95 th percentile] difference in seasonally averaged water age (days)	
	<u>Apr to Sep</u> <u>Active</u>	<u>Oct to Mar</u> <u>Dormant</u>	<u>Apr to Sep</u> <u>Active</u>	<u>Oct to Mar</u> <u>Dormant</u>
<u>Outlet stream discharge</u>	<u>a)</u>		<u>b)</u>	
Baseline	647 [355, 989]	484 [292, 758]	-	-
Thicket	763 [439, 1527]	610 [373, 1136]	164 [19, 613]	128 [22, 440]
Old open forest	643 [367, 1103]	497 [298, 854]	30 [-29, 141]	24 [-17, 108]

Formatted Table

Formatted: Font: Not Italic, Underline

<u>Lateral groundwater fluxes</u>	e)		d)	
Baseline	521 [375, 774]	441 [305, 672]	-	-
Thicket	690 [469, 1202]	590 [410, 999]	196 [18, 476]	163 [20, 405]
Old open forest	545 [397, 824]	465 [337, 736]	28 [-30, 99]	26 [-22, 89]
<u>Soil layer L1 (L1)</u>	e)		f)	
Baseline	266 [166, 556]	293 [173, 565]	-	-
Thicket	301 [192, 696]	288 [183, 636]	35 [-8, 193]	8 [-11, 114]
Old open forest	271 [174, 565]	291 [179, 581]	6 [-9, 43]	5 [-6, 32]
<u>Soil evaporation</u>	g)		h)	
Baseline	276 [168, 673]	281 [181, 586]	-	-
Thicket	395 [253, 1039]	329 [218, 823]	124 [12, 502]	62 [-4, 349]
Old open forest	291 [189, 683]	299 [193, 614]	12 [-42, 96]	12 [-9, 71]
<u>Transpiration</u>	i)		j)	
Baseline	353 [206, 737]	365 [227, 780]	-	-
Thicket	361 [204, 642]	309 [208, 450]	11 [-106, 71]	-54 [-336, 10]
Old open forest	409 [219, 780]	414 [237, 727]	41 [-14, 89]	26 [-103, 83]

Formatted: Font: Not Italic, Underline

Formatted: Left

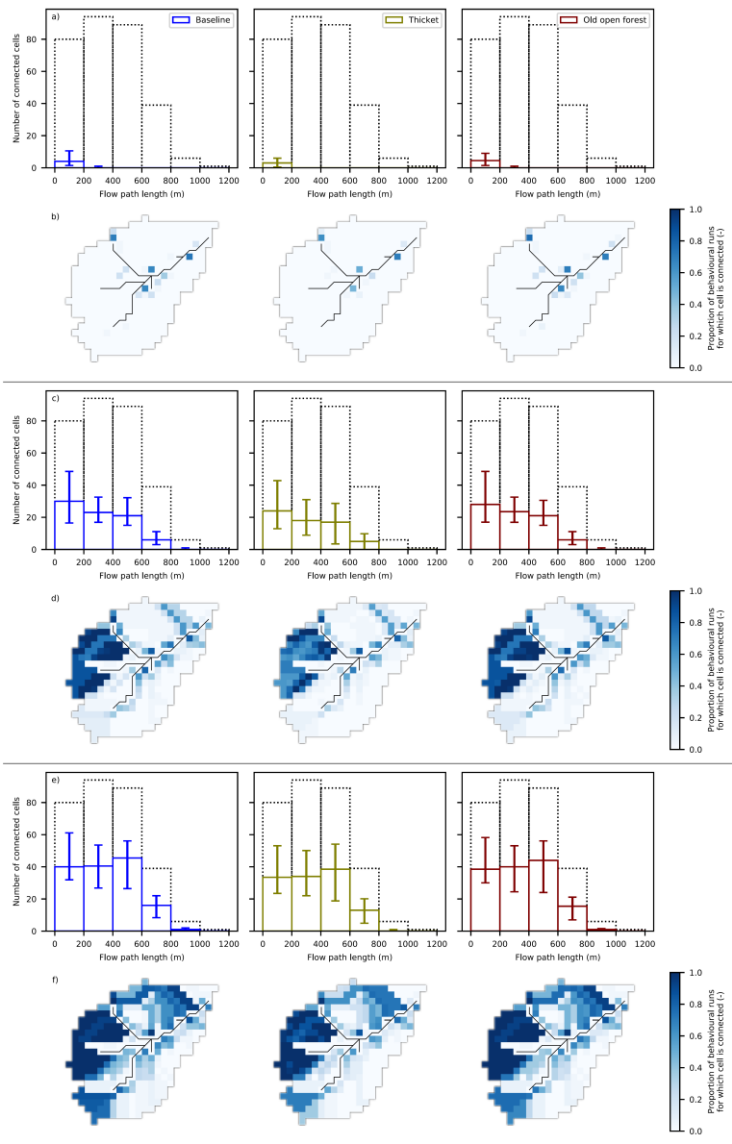
Formatted: Font: Not Italic, Underline

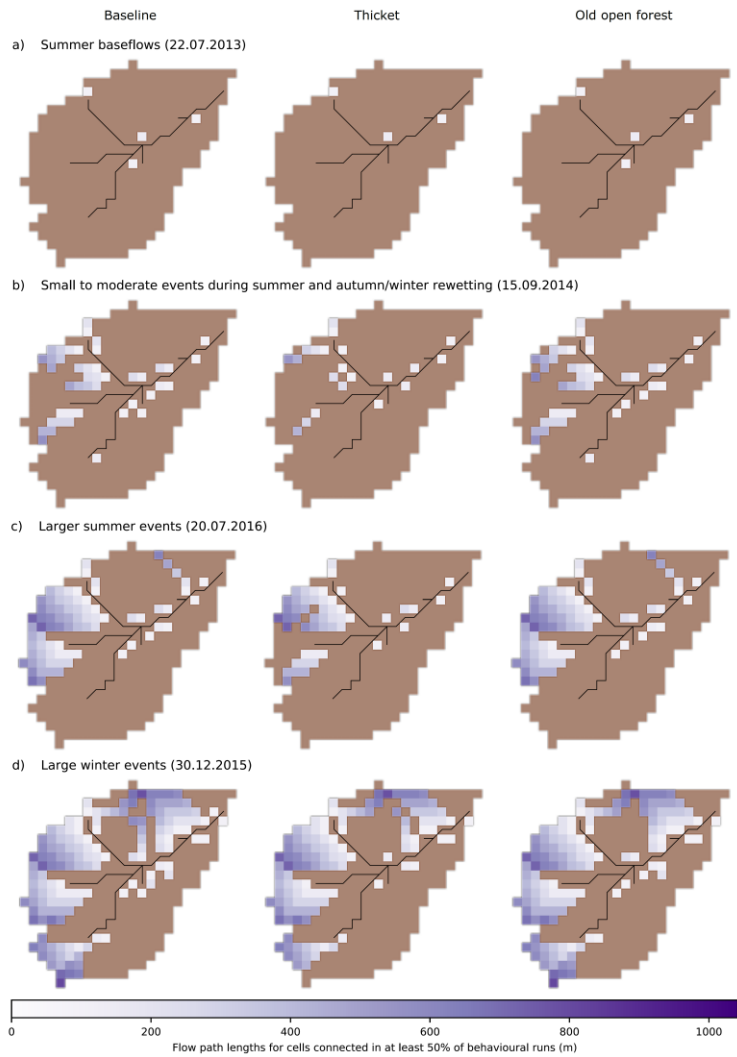
4.7 Changes to hydrological connectivity

For the considered flow conditions, Fig. 9 summarises spatial patterns of hydrological connectivity that were simulated by at least 50% of the behavioural model runs dynamics for the three investigated dates. Histograms show the number of cells with given flow path lengths that were connected to the stream for each scenario, whilst maps show the proportion of behavioural model runs for which a cell was simulated as connected. On 22 July 2013, baseline connectivity during summer baseflows was generally only established for a limited (~5% of potential) number of cells close to the stream; for 22 July 2013 only ~1% of cells were connected due to particularly dry summer conditions at this time (Fig. 9a). (Fig. 9a-b), reflecting the dry summer conditions. In the thicket scenario, the spatial extent of connectivity became even more limited, though saturation in the valley bottom was maintained (Fig. 9a-b). Regeneration of old open forest did not substantially affect have a substantial

~~effect on~~ connectivity dynamics; indeed, this was the case for all flow conditions considered. The catchment had a wetter baseline state for small to moderate summer and autumn/winter rewetting events, with 14% of cells being connected on 15 September 2014 (Fig. 9b). This reflected greater connectivity in the valley bottom and establishment of longer flow paths (up to 600 m) in the west of the catchment. These flow paths tended to become shorter in the thicket scenario; along with slightly less connectivity in the valley bottom, this caused a 52% reduction in cells that were connected to the stream. Stronger connectivity and longer flow paths

545





550 **Figure 9:** For the end of a prolonged summer dry-period (22 July 2013), a) A histogram showing the number of cells with different flow path lengths that were connected to the stream via overland flow, and b) A map showing the proportion of behavioural runs for which each cell was connected to the stream via overland flow. c-d) Are the same for the height of a late summer wet period (10

555 August 2014) whilst e-f) are for a 100-year return period flood (30 December 2015). Dashed lines in the histograms indicate the total number of cells in the catchment with a given flow path length to the stream. Spatial patterns of hydrological connectivity simulated in at least 50% of behavioural model runs for dates representative of a) Summer baseflows; b) Small to moderate events during summer and autumn/winter rewetting; c) Larger summer events; and d) Large winter events. Disconnected cells are shown in brown.

560 (up to 800 m) in the west of the catchment and establishment of a long flow path down the northern hillslope led to 25% of cells being connected in the representative larger summer event on 20 July 2016 (Fig. 9c). Whilst some cells with longer flow paths did disconnect in the thicket scenario, the largest reductions in connectivity resulted from disconnection of cells with more moderate flow path lengths (up to 600 m) in the west of the catchment. Despite this, however, large connected areas were maintained in both the west of the catchment and valley bottom, leading to a 36% reduction in connectivity overall. Large winter events showed the greatest baseline connectivity, with 48% of cells connected to the stream on 30 December 2015 (Fig. 9d). This reflected greater

565 The catchment had a much wetter baseline state on 10 August 2014 with, on average, 26% of cells connected to the stream. Connectivity was concentrated in the west of the catchment and along isolated segments of the north and south hillslopes (Fig. 9d). Connected cells generally had flow path lengths of up to 600 m, although more distant cells could also be connected (Fig. 9e). In the thicket scenario, the proportional decrease in the median connectivity of cells with flow paths lengths between 400 and 600 m was less than for cells closer to or further from the stream (Fig. 9e). This reflected persistence of longer connected flow paths predominantly in the west of the catchment but also on the northern hillslope where there is an ephemeral GW seepage track (Fig. 9d; Scheliga et al., 2019). However, the likelihood of cells in the west and also south of the catchment being connected in a behavioural model run did decline (Fig. 9d). In the old open forest scenario, the distribution of connected cells was again very similar to the baseline.

575 Even greater baseline connectivity was simulated for 30 December 2015 with, on average, 46% of cells connected to the stream (Fig. 9e). The more consistent establishment of connectivity on the northern hillslope and in the SW-south-west headwater that also increased the number of connected cells with moderate to long (>400 to 1000 m) flow path lengths (Fig. 9e-f). Spatial patterns of connectivity were similar overall in the thicket scenario, with the main notable changes being reduced connectivity in the south-west headwaters and disconnection of specific flow paths on the northern hillslopes due to more limited OLF generation from some riparian cells. The podzols in the south remained least connected, though the connected area did extend further upslope (Fig. 9f). In the thicket scenario, spatial patterns of connectivity were similar overall and cells with longer flow paths could still be connected (Fig. 9e-f). However, the median number of connected cells decreased for all flow path lengths (Fig. 9e), with reductions in connectivity most notable in the SW (Fig. 9f). There were also areas where reduced OLF generation from riparian cells substantially limited the connectivity potential of upslope cells (e.g. around the headwater confluences; Figs. 7a and 9f). Connectivity in the old open forest scenario was again comparable to the baseline. These changes led to just a 16% reduction in the total number of cells connected to the stream.

5 Discussion

5.1 ~~Simulated~~ The effects of natural forest regeneration on “blue” and “green” water partitioning

590 Previous studies investigating the hydrological consequences of changes in forest cover have often sought to understand how conversion and management of land for commercial forestry affects aggregated metrics of catchment hydrological functioning (Ellison et al., 2017; Filoso et al., 2017), especially so in the UK context (Marc and Robinson, 2007). Consequently, findings may not be transferable to the case of passively managed natural forest regeneration that is the goal of rewilding efforts in degraded landscapes such as the Scottish Highlands (zu Ermgassen et al., 2018). Therefore, using the EcH₂O-iso model, we investigated the ecohydrological consequences of natural pinewood regeneration for the BB catchment in Scotland by comparing simulated present-day baseline conditions with two land cover change scenarios representing different stages of forest regeneration (thicket and old open forest).
595

The overall skill of the model in ~~simulating capturing the dynamics of~~ diverse ecohydrological and isotope datasets (Table 2; Fig. 3) helped provide confidence in its ability to simulate plausible realisations of catchment functioning. However, despite the rich calibration dataset, larger uncertainties persisted in some model outputs (e.g. water ages; Fig. 5d). This likely reflected a combination of several factors, including the extent to which available data can constrain specific details of individual processes simulated by complex models alongside more general features of catchment functioning (e.g. surface water vs. GW dominated; Holmes et al., 2020; Neill et al., 2020), limitations in the information content of certain datasets (e.g. extent to which isotopes constrain GW fluxes older than 5 years; Stewart et al., 2010), and differences in scale between observations, real-world processes and model resolution (Smith et al., 2021). Such factors are commonly associated with complex, spatially-distributed models (e.g. Beven, 2006), and their persistence here indicates the need for continued research into how such models can best be constrained for their necessary use in studying issues such as land cover change (Fatichi et al., 2016b). Nonetheless, the overall skill of EcH₂O-iso, alongside consistency of simulated “blue” fluxes with independently-derived conceptual models of the BB catchment (Ala-aho et al., 2017; Tetzlaff et al., 2014) and a previous successful application to the catchment where isotope data were used for independent validation (Kuppel et al., 2018a), meant that the model could still serve as a useful tool for simulating regeneration scenarios.
600
605
610

~~, its past independent validation in the BB using isotope data (Kuppel et al., 2018a), and consistency of simulated “blue” fluxes with conceptual models of the BB derived from past empirical (Tetzlaff et al., 2014) and independent modelling (Ala-aho et al., 2017) studies, gave confidence in using EcH₂O-iso for simulating the effects of forest regeneration.~~

615 Our major finding was that dynamics of water partitioning deviated most strongly from the baseline during early stages of regeneration with ~~likely potential for~~ recovery as the forest matured and opened out. The latter is consistent with previous work in plantations that has suggested the hydrological impacts of forests will lessen as they mature (e.g. Delzon and Loustau, 2005; Du et al., 2016; Marc and Robinson, 2007). During the thicket stage, simulated increases in interception evaporation

Formatted: Subscript

620 principally drove changes to water partitioning (Table 3). This was facilitated by the greater simulated interception storage capacity of the thicket forest (Fig. 4b) and is consistent with findings in relation to commercial plantations (e.g. Birkinshaw et al., 2014; Farley et al., 2005; Johnson, 1990). Interestingly, the greatest increase in interception evaporation occurred during the dormant season, resulting in a proportionally larger increase in “green” fluxes at this time rather than during the ~~more biologically active period season~~. This has been observed in other studies where the canopy is wet for prolonged periods over
625 winter (e.g. Birkinshaw et al., 2014; Peng et al., 2016). ~~It further seems to reinforce the notion that higher rates of interception evaporation can be facilitated in periods of reduced net radiation through, and seems to reinforce the importance of~~ enhanced turbulent airflows over forests and sensible heat exchanges between the canopy and atmosphere, ~~in facilitating high interception evaporation when available net radiation is reduced~~ (c.f. Stewart, 1977; Gash and Stewart, 1977). To a lesser degree, simulated increases in summer transpiration also contributed to greater apportionment of water to “green” fluxes (Table
630 3). The reduced importance of increased transpiration relative to interception evaporation has been observed elsewhere for coniferous forests (Farley et al., 2005; Marc and Robinson, 2007).

Increased losses to interception evaporation and transpiration were slightly compensated by a reduction in simulated soil evaporation (Table 3) that was also reflected in more isotopically depleted summer stream flows (Fig. 5c). Overall, however,
635 availability of water for ~~“blue”-GW recharge and streamflow fluxes~~ was reduced (Table 3). ~~This notably led to simulated summer baseflows becoming increasingly reduced and further caused reductions in the magnitude of small to moderate events both in summer and during the autumn/winter rewetting period, notably resulting in lower simulated summer baseflows~~ (Fig. 5b; c.f. Iacob et al., 2017). ~~These changes likely reflected greater storage deficits developing in the catchment through summer due to increased transpiration demand in the active season (Fig. 8b) amplifying the effect of reductions in GW recharge on the hillslopes (particularly during the previous dormant season) and, consequently, downslope GW subsidies to the valley bottom. This likely reflected increased transpiration demand (Fig. 8b) amplifying the effect of reduced GW subsidies from regenerating areas on the podzols and rankers to the valley bottom (Fig. 7d-e; Brown et al., 2005; Calder, 1993). In the BB catchment, these subsidies~~ ~~In the BB, these subsidies~~ are crucial for recharging GW stores in drift deposits that sustain baseflow conditions (Blumstock et al., 2016; Kuppel et al., 2020) and further help maintain saturated conditions in the valley bottom (Tetzlaff et al., 2014). ~~To overcome the increased deficit, a greater amount of precipitation was then needed in the dormant season to rewet the catchment despite losses to interception evaporation also being increased at this time (Fig. 8d). Consequently, full rewetting was delayed until a sufficiently large winter rainfall event occurred, with smaller events prior to this demonstrating reduced magnitudes. This ability of local changes in flux partitioning to have significant consequences over extended areas, particularly in winter when GW recharge is usually highest (Table 3; Blumstock et al., 2016; Kuppel et al., 2020). This finding is significant as it~~ reinforces the need to consider the wider hydrological consequences of regeneration occurring in specific
640 areas-locations such that the “right tree [is planted] in the right place” (Forestry Commission Scotland, 2010). ~~The lesser impact of thicket forest on the simulated magnitude of high flows suggests that increases in storage capacities (Fig. 4) and “green” water fluxes (Table 3) were insufficient to overcome the combined influences of antecedent conditions and precipitation inputs~~

655 ~~that led to the largest events modelled here (Fig. 5b). Greater consistency in simulated high flows suggests that increases in storage capacities (Fig. 4) and “green” water fluxes (Table 3) for the thicket scenario were insufficient to moderate the combined influences of antecedent conditions and precipitation inputs that led to the largest events modelled here (Fig. 5b). This is consistent with previous work showing that forest regeneration may have a limited impact on the magnitudes of the largest flood events (Calder et al., 2007; Jacob et al., 2017; Soulsby et al., 2017). It is possible that the frequency of such events could be reduced; however, assessment would require a longer run of data to derive flow duration curves (Alila et al., 2009).~~

660 ~~Greater alignment between simulated water partitioning dynamics in the baseline and old open forest scenarios (Table 3; Figs. 7 and 8) was consistent with previous work in plantations that has suggested the hydrological impacts of forests will lessen as they mature (e.g. Delzon and Loustau, 2005; Du et al., 2016; Marc and Robinson, 2007). However, the simulated drying out of the valley bottom in the thicket scenario (Fig. 7) raises the question as to whether pinewoods could progressively encroach downslope to replace the bog woodland on the peaty gleys and, eventually, the *Sphagnum* on the peat. This would entail the creation of a positive feedback loop whereby establishment of forest reduces downslope waterlogging to permit further forest expansion and, ultimately, the shift of the catchment into a different state of dynamic equilibrium (c.f. Rodriguez-Iturbe, 2000; Peterson and Western, 2014; Peterson et al., 2009). In turn, this could prolong the changes to water partitioning simulated for the thicket scenario.~~

670 5.2 Storage-flux dynamics ~~during of regenerating forest~~ **regeneration** ~~s~~ as revealed by water ages

Given uncertainty in simulated water ages, it is difficult to definitively conclude how forest regeneration would affect source waters of “blue” and “green” fluxes. In general, increased losses of zero-aged precipitation to interception evaporation in the thicket scenario created a tendency for slower turnover of below-canopy water that was particularly expressed in the older average ages of soil ~~water and~~ evaporation, lateral GW flows and streamwater (Table 4). ~~The greater increase in soil evaporation—Soil evaporation being age older relative to than soil water in L1 age—likely reflected reduced evaporation of younger water from the freely draining soils on the hillslopes increasing and the consequent increased the dominant influence of older water evaporated evaporation of well-mixed, older water~~ from the valley bottom (Figs. 6 and 8c; Sprenger et al., 2017; Tetzlaff et al., 2014). ~~It may also indicate that periods of greatest atmospheric evaporative demand were satisfied by soil waters from the valley bottom on which the aging effects of older upslope GW subsidies were most imprinted.~~ Average streamflow ages reflected the potential for low/moderate flows to consist of older water (Fig. 5d) which, in turn, indicated increased relative contributions of GW that was itself older. Streamwater ages remaining relatively young during higher flows supports the previous assertion that regeneration did not prevent activation of rapid OLF paths in larger events. Average ages of these fluxes were generally restored in the old open forest scenario (Table 4).

690 The similarity in average transpiration ages amongst simulated scenarios contrasts with ~~other~~ studies in drier catchments that have suggested forests and other vegetation covers, such as grassland, transpire water with differing age characteristics (Douinot et al., 2019; Smith et al., 2020). ~~This suggests that the wet, low energy climate of the BB and generally well-mixed nature of hydrological stores allows the catchment to accommodate increased “use” of water by forests more readily than drier environments with less retentive soils in which forest water uptake must be satisfied by younger, more recent inputs of water that increases their susceptibility to drought-induced water stress (Kleine et al., 2020; Smith et al., 2020). Transpiration becoming younger than soil evaporation in the thicket scenario reflected changes in the spatial patterns of both fluxes (Fig. 8), with increased transpiration of younger water from the hillslopes relative to older water from the valley bottom helping to further accentuate the aforementioned effect of changes to soil evaporation.~~ However, the greater uptake of deeper, older water
695 by thicket pine and the slower turnover of water on the hillslopes due to increased losses to interception evaporation likely caused transpiration ages to remain generally comparable to the baseline, with only 95th percentile average ages showing a noticeable reduction (Table 4). Small increases in the median of average transpiration ages for the old open forest scenario likely reflected old open pines transpiring deeper water from the hillslopes (Fig. 4a) but also the slight reduction in the magnitude of these fluxes relative to older transpiration fluxes in the valley bottom (Fig. 8b). Overall, transpiration ages
700 remaining on the order of months to years implies that moisture carried over from previous seasons would be sufficient to satisfy forest transpiration demands (c.f. Allen et al., 2019; Brinkmann et al., 2018; Kuppel et al., 2020). This suggests that the wet, low energy climate of the BB catchment and generally well-mixed nature of hydrological stores allows increased “use” of water by forests to be more readily accommodated than in drier environments with less retentive soils. In the latter, water uptake must be satisfied by younger, more recent inputs of water, increasing the susceptibility of forests to drought-induced
705 water stress (Kleine et al., 2020; Smith et al., 2020).

Despite the associated uncertainties, these findings demonstrate how consideration of water ages can enhance understanding of the spatio-temporal aspects of storage-flux interactions and, importantly, their sensitivity to change (Sprenger et al., 2019). In addition, inferences can also be made that have implications for wider ecosystem resilience. For instance, the reduced
710 magnitude of summer low to moderate flows in the thicket scenario could negatively affect the ability of Atlantic salmon to access important spawning areas (Moir et al., 1998). However, greater contributions of GW to these flows implied by older water ages may equally be beneficial through mitigating extreme temperature fluctuations in the stream to which salmon are sensitive (Glover et al., 2020).

Reduced 95th percentile average ages in the thicket scenario (especially for Oct-Mar) may have partially reflected greater young water contributions to forest transpiration owing to increased percolation of younger soil water from L1 to L2 as a consequence of enhanced root water uptake from the latter (c.f. Table S2; Fig. 4a). However, that transpiration ages remained on the order of months to years implies that moisture carried over from previous seasons was sufficient to satisfy transpiration demand (c.f. Allen et al., 2019; Brinkmann et al., 2018; Kuppel et al., 2020). Slightly older median transpiration ages in the old open forest

Formatted: Superscript

720 scenario likely reflected increased uptake from the lower soil layers (Fig. 4a) combined with transpiration fluxes that had a more limited effect on water turnover rates relative to the thicket scenario (Table 3i).

5.3 Implications of regeneration for hydrological source areas and connectivity

The effect of forest regeneration on hydrological source areas and connectivity can be informative regarding its use as a nature-based solution to management issues of water quantity and quality. Consistent with inferences from the discharge timeseries (Fig. 5b), establishment of thicket forest most strongly affected spatial patterns of connectivity for small to moderate events in summer and during autumn/winter rewetting the examined low and moderate summer flow events (Fig. 9ba-d). Meanwhile, whilst only relatively minor changes were simulated more limited for a larger events in summer and winter, in particular event (Fig. 9e-fc-d). Interestingly, whilst the shortening of connected flow paths in smaller summer/rewetting events likely reflected the enhanced dry state of the catchment at this time (see Sect. 5.1), the disconnection of only limited and specific flow paths or areas (e.g. south-west headwaters) in larger events implies daily average OLF was simulated to reduce across much of the catchment (Fig. 7a), examination of event based connectivity revealed that only specific flow paths or areas of the catchment (e.g. SW headwaters) were likely to fully disconnect from the stream. This highlights that certain areas-parts of the catchment may be more sensitive to forest establishment. This and could be useful for managing regeneration to minimise/maximise its impact on certain flow types (Collentine and Futter, 2018; Iacob et al., 2017). The inability of regeneration to fully interrupt connectivity between the hillslopes and riparian zone, however, likely explains why high flow magnitudes tended to be maintained across the simulated scenarios. This is because such connectivity is a major driver of non-linear storm flow responses in catchments such as the BB (Birkel et al., 2015; Soulsby et al., 2015; Stockinger et al., 2014), under increasingly wet catchment states additionally offers an explanation as to why high flow magnitudes tended to be maintained across the simulated scenarios. This may also limit the effectiveness of forest regeneration in regulating certain water quality parameters by reducing redistribution of contaminants from the hillslope to the riparian zone (e.g. faecal indicator organisms – Neill et al., 2019).

745 Whilst these findings imply that forest regeneration may “slow the flow” (Fig. 7a) but not fully disconnect surface flow paths from the stream under increasingly wet conditions (Fig. 9), it is likely that simulated changes to connectivity are conservative. This is because increases in surface roughness and detention storage caused by vegetation change cannot presently be simulated in EcH₂O-iso; however, these factors may also affect connectivity alongside changes to water flux partitioning (Collentine and Futter, 2018; Turnbull and Wainwright, 2019).

5.4 Uncertainty in the forest regeneration scenarios

750 In this work, the thicket and old open forest scenarios represented earlier and later stages of regeneration where trees are most
and least dense, respectively. Consequently, their simulated ecohydrological consequences likely indicate the extremes of what
could result from natural pinewood regeneration. However, uncertainty surrounds the actual trajectory of regeneration that will
result from rewilding activities taking place today, given the decadal timescale of regeneration. For instance, future climate
projections for Scotland suggest that rainfall will decrease in summer and increase in winter, whilst temperatures will rise
755 overall (Capell et al., 2014; Werrity and Sugden, 2012). Understanding how the interplay of these changes will affect
regeneration trajectories is complex, as warmer and drier summers could limit the extent to which increased transpiration
demands can be met during earlier stages of regeneration, whilst wetter winters may help to counteract the effects of increased
dormant-season losses to interception evaporation simulated here (Table 3; Fig. 8d). Assuming forests can reach later stages
of regeneration, management decisions may further influence the final structural characteristics of older forests. Even when
760 the idea of rewilding is adopted, there are still debates over exactly what it means and what its ultimate end goal should be
(Deary and Warren, 2017). For example, regeneration of old open forest would likely result from one rewilding trajectory (see
Sect. 3.4), whilst another trajectory that is more “hands-off” may lead to later stages of regeneration resembling high crown
forests containing taller and slightly denser trees than old open forests (Fig. S1; Summers et al., 1997; 2008). Overall, the more
open nature of both end points relative to forests at earlier stages of regeneration likely means that ecohydrological flux and
765 age restoration will occur to some extent as regenerating forests mature; however, the old open forest scenario simulated here
likely represents a “best case” outcome.

A final source of uncertainty arises from the Greater alignment between simulated water partitioning dynamics in the baseline
and old open forest scenarios (Table 3; Figs. 7 and 8) was consistent with previous work in plantations that has suggested the
770 hydrological impacts of forests will lessen as they mature (e.g. Delzon and Loustau, 2005; Du et al., 2016; Mare and Robinson,
2007). However, the simulated drying out of the valley bottom in the thicket scenario (Fig. 7)-. This raises the question as to
whether pinewoods could progressively encroach downslope to replace the bog woodland on the peaty gleys and, eventually,
the *Sphagnum* on the peat. This would entail the creation of a positive feedback loop whereby establishment of forest reduces
downslope waterlogging to permit further forest expansion until eventually a state is reached in which older forest is present
775 on the hillslopes and younger forest in the valley bottom. Establishment of such a feedback would likely ~~and, ultimately, the~~
shift of the catchment into a different state of dynamic equilibrium (c.f. Rodriguez-Iturbe, 2000; Peterson and Western, 2014;
Peterson et al., 2009) and potentially give rise to quite different spatial configurations of regeneration compared to the one
considered here.). In turn, this could prolong the changes to water partitioning simulated for the thicket scenario.
Ecohydrological models are likely well-placed to explore such possibilities; however, this would be contingent on processes
780 such as seed dispersal and species competition being conceptualised in models such as EcH₂O-iso (c.f. Fatichi et al., 2016a).

6 Conclusions and wider implications

In this work, we demonstrated that the ecohydrological consequences of natural forest regeneration on degraded land depend on the structural characteristics of the forest at different stages of development. We also showed how hydrological functioning of the wider catchment can be affected by spatial changes in water flux partitioning caused by regeneration in specific areas (e.g. hillslopes). Consequently, land cover change studies need to move beyond simply considering forested vs. non-forested scenarios to provide a robust evidence base for management decisions seeking to balance regeneration/rewilding with other ecosystem services. Early stages of regeneration ~~are~~ were suggested to have the most significant ecohydrological consequences/effects on catchment hydrology with the catchment entering a drier state and low to moderate flows during summer and autumn/winter rewetting demonstrating reduced magnitudes and more limited hydrological connectivity. Higher flows were less impacted, however, reinforcing the notion that forest regeneration may become less effective as a nature-based solution to issues of water quantity and quality under increasingly wet conditions. The overall drier catchment state could - ~~The drier catchment state and reduced low/moderate flows may have~~ have negative implications for fire risk (Turetsky et al., 2015), aquatic ecosystems, (e.g. those supporting Atlantic Salmon populations — Moir et al., 1998) and downstream services like drinking water provision. However, recovery of flux partitioning and water ages during later stages of regeneration ~~implies~~ implied that such issues ~~may~~ could be transient, with landscapes covered by older forest ~~perhaps~~ perhaps able to support pre-existing ecosystem services whilst improving biodiversity. ~~Potential effectiveness of regeneration as a nature-based solution to water quantity and quality issues appeared greatest during the thicket stage for dry to moderately wet catchment states. Whilst the impact on high flow magnitudes was limited for events simulated here, it is possible that the frequency of such events could be reduced; however, assessment would require a longer run of data to derive flow duration curves (Alila et al., 2009).~~

Our work also ~~highlights~~ highlighted the ~~value~~ merits of using tracer-aided ecohydrological models as tools for land cover change investigations. In particular, processes such as enhanced ~~forest~~ interception evaporation ~~from forests~~ could be explicitly simulated. Additionally, tracking of water ages permitted greater insight into the spatio-temporal dynamics of storage-flux interactions and their resilience to forest regeneration. Despite calibration to a rich dataset, however, larger uncertainties still persisted in some model outputs. Therefore, future work could usefully look at what other types of data may help improve constraint of complex models such as EcH₂O-iso. Alongside this, use of tracer-aided ecohydrological models could be further enhanced through a better understanding of simulated (e.f. Calder, 1976), whilst successful reproduction of diverse ecohydrological and isotope observations increased confidence in simulated catchment internal functioning. Such models also have further potential. In the first instance, incorporating temporal variability in soil characteristics could provide a more complete understanding of the ecohydrological consequences of land cover change; however, there remains a need to better characterise how soil properties change in response/respond to land cover changes. (Areher et al., 2013; Chandler et al., 2018)

Formatted: Subscript

and ~~to understand how the this effect this has on translates into changes in~~ “effective” model parameters ~~(Seibert and van~~
815 ~~Meerveld, 2016), and through conceptualisation of processes such as seed dispersal and species competition that would allow~~
~~simulation of dynamic feedbacks that could alter trajectories of change.~~ Second, whilst static snapshots were used to simulate
stages of land cover change, ecohydrological models could potentially explore the development of dynamic feedbacks that
could alter trajectories of change (e.g. forest encroachment into the valley bottom; c.f. Perino et al., 2019; Scott and Prinsloo,
2008). For scenarios of vegetation change, this would be contingent on processes such as seed dispersal and species
820 ~~competition being conceptualised in models such as EcH₂O iso (c.f. Fatichi et al., 2016).~~

Code and data availability

~~Data are available from the corresponding author on request.~~ The model code for EcH₂O-iso is available at:
https://bitbucket.org/sylka/ech2o_iso/src/master_2.0/. Files and scripts needed to reproduce and analyse model outputs -are
825 available via the University of Aberdeen PURE repository: <https://doi.org/10.20392/045cd572-ecc8-4dfd-b003-c0d0c621510e>.

Author contribution

AJN and CS formulated the overarching research goals and approach of the paper. AJN, in discussion with CS, carried out
model setup, calibration, scenario analysis and visualisation of results, using the EcH₂O-iso model developed as part of work
by DT, CS and MPM. All authors contributed to interpretation of results. AJN drafted the initial manuscript with all co-authors
830 extensively contributing to its evolution. CS, along with CB and MPM, secured funding for the ISOLAND project, and was
responsible for oversight of research activities. DTs VeWa project facilitated original data collection for the Bruntland Burn.

Competing interests

The authors declare that they have no conflict of interest.

Acknowledgements

835 Funding for this work was provided by the Leverhulme Trust ISOLAND project (RPG 2018 375) and the European Research
Council VeWa project (VeWa project GA 335910). Many thanks go to past members of the VeWa project who were involved
in collection and curation of data for the Bruntland Burn catchment. All model runs were carried out on the Maxwell High
Performance Cluster (HPC) funded and maintained by the University of Aberdeen.

References

- 840 Aerts, R., Bakker, C., De Caluwe, H., 1992. Root turnover as determinant of the cycling of C, N, and P in a dry heathland ecosystem. *Biogeochemistry* 15: 175-190. DOI: 10.1007/BF00002935
- Ala-aho, P., Soulsby, C., Wang, H., Tetzlaff, D., 2017. Integrated surface-subsurface model to investigate the role of groundwater in headwater catchment runoff generation: A minimalist approach to parameterisation. *Journal of Hydrology* 547: 664-677. DOI: 10.1016/j.jhydrol.2017.02.023
- 845 Alila, Y., Kuraš, P.K., Schnorbus, M., Hudson, R., 2009. Forests and floods: A new paradigm sheds light on age-old controversies. *Water Resources Research* 45: W08416. DOI: 10.1029/2008WR007207
- Allen, S.T., Kirchner, J.W., Braun, S., Seigwolf, R.T.W., Goldsmith, G.R., 2019. Seasonal origins of water used by trees. *Hydrology and Earth System Sciences* 23: 1199-1210. DOI: 10.5194/hess-23-1199-2019
- Archer, N.A.L., Bonell, M., Coles, N., MacDonald, A.M., Auton, C.A., Stevenson, R., 2013. Soil characteristics and landcover relationships on soil hydraulic conductivity at a hillslope scale: A view towards local flood management. *Journal of Hydrology* 497: 208-222. DOI: 10.1016/j.jhydrol.2013.05.043
- 850 Bergstrom, A., Jencso, K., McGlynn, B., 2016. Spatiotemporal processes that contribute to hydrologic exchange between hillslopes, valley bottoms, and streams. *Water Resources Research* 52: 4628-4645. DOI: 10.1002/2015WR017972
- Beven, K., 2006. A manifesto for the equifinality thesis. *Journal of Hydrology* 320: 18-36. DOI: 10.1016/j.jhydrol.2005.07.007
- 855 Birkel, C., Soulsby, C., 2015. Advancing tracer-aided rainfall-runoff modelling: a review of progress, problems and unrealised potential. *Hydrological Processes* 29: 5227-5240. DOI: 10.1002/hyp.10594
- Birkel, C., Tetzlaff, D., Dunn, S.M., Soulsby, C., 2010. Towards a simple dynamic process conceptualization in rainfall-runoff models using multi-criteria calibration and tracers in temperate, upland catchments. *Hydrological Processes* 24, 260-275. DOI: 10.1002/hyp.7478
- 860 [Birkel, C., Soulsby, C., Tetzlaff, D., 2011. Modelling catchment-scale water storage dynamics: reconciling dynamic storage with tracer-inferred passive storage. *Hydrological Processes* 25: 3924-393. DOI: 10.1002/hyp.8201](#)
- Birkel, C., Soulsby, C., Tetzlaff, D., 2015. Conceptual modelling to assess how the interplay of hydrological connectivity, catchment storage and tracer dynamics controls nonstationary water age estimates. *Hydrological Processes* 29: 2956-2969. DOI: 10.1002/hyp.10414
- 865 Birkinshaw, S.J., Bathurst, J.C., Robinson, M., 2014. 45 years of non-stationary hydrology over a forest plantation growth cycle, Coalburn catchment, Northern England. *Journal of Hydrology* 519: 559-573. DOI: 10.1016/j.jhydrol.2014.07.050
- Blumstock, M., Tetzlaff, D., Malcolm, I.A., Nuetzmann, G., Soulsby, C., 2015. Baseflow dynamics: Multi-tracer surveys to assess variable groundwater contributions to montane streams under low flows. *Journal of Hydrology* 527, 1021-1033. DOI: 10.1016/j.jhydrol.2015.05.019

- 870 Blumstock, M., Tetzlaff, D., Dick, J.J., Nuetzmann, G., Soulsby, C., 2016. Spatial organisation of groundwater dynamics and streamflow response from different hydropedological units in a montane catchment. *Hydrological Processes* 30, 3735-3753. DOI: 10.1002/hyp.10848
- Bonan, G.B., Forests and Climate Change: Forcings, Feedbacks, and the Climate Benefits of Forests. *Science* 320: 1444-1449. DOI: 10.1126/science.1155121
- 875 Bosch, J.M., Hewlett, J.D., 1982. A review of catchment experiments to determine the effect of begetation changes on water yield and evapotranspiration. *Journal of Hydrology* 55: 3-23. DOI: 10.1016/0022-1694(82)90117-2
- Brinkmann, N., Seeger, S., Weiler, M., Buchmann, N., Eugster, W., Kahmen, A., 2018. Employing stable isotopes to determine the residence times of soil water and the temporal origin of water taken up by *Fagus sylvatica* and *Picea abies* in a temperate forest. *New Phytologist* 219: 1300-1313. DOI: 10.1111/nph.15255
- 880 Brown, A.E., Zhang, L., McMahon, T.A., Western, A.W., Vertessy, R.A., 2005. A review of paired catchment studies for determining changes in water yield resulting from alterations in vegetation. *Journal of Hydrology* 310: 28-61. DOI: 10.1016/j.jhydrol.2004.12.010
- ~~Calder, I.R., 1976. The measurement of water losses from a forested area using a "natural" lysimeter. *Journal of Hydrology* 30: 311-325. DOI: 10.1016/0022-1694(76)90115-3~~
- 885 Calder, I.R., 1993. The Balquhiddy catchment water balance and process experiment results in context what do they reveal? *Journal of Hydrology* 145: 467-477. DOI: 10.1016/0022-1694(93)90070-P
- Calder, I.R., Smyle, J., Bruce, A., 2007. Debate over flood-proofing effects of planting forests. *Nature* 450: 945. DOI: 10.1038/450945b
- ~~Capell, R., Tetzlaff, D., Essery, R., Soulsby, C., 2014. Projecting climate change impacts on stream flow regimes with tracer-aided runoff models - Preliminary assessment of heterogeneity at the mesoscale. *Hydrological Processes* 28: 545-558. DOI: 10.1002/hyp.9612~~
- 890 Chai, T., Draxler, R.R., 2014. Root mean square error (RMSE) or mean absolute error (MAE)? – Arguments against avoiding RMSE in the literature. *Geoscientific Model Development* 7: 1247-1250. DOI: 10.5194/gmd-7-1247-2014
- Chandler, K.R., Stevens, C.J., Binley, A., Keith, A.M., 2018. Influence of tree species and forest land use on soil hydraulic conductivity and implications for surface runoff generation. *Geoderma* 310: 120-127. DOI: 10.1016/j.geoderma.2017.08.01
- 895 Chappell, N., Stobbs, A., Terman, L., Williams, A., 1996. Localised impact of Sitka spruce (*Picea sitchensis* (Bong.) Carr.) on soil permeability. *Plant and Soil* 182: 157-169. DOI: 10.1007/BF00011004
- Coble, A.A., Barnard, H., Du, E., Johnson, S., Jones, J., Keppeler, E., Kwon, H., Link, T.E., Penaluna, B., Reiter, M., River, M., Puettmann, K., Wagenbrenner, J., 2020. Long-term hydrological response to forest harvest during seasonal low flow: Potential implications for current forest practices. *Science of the Total Environment* 730: 138926. DOI: 10.1016/j.scitotenv.2020.138926
- 900 Collentine, D., Futter, M.N., 2018. Realising the potential of natural water retention measures in catchment flood management: trade-offs and matching interests. *Journal of Flood Risk Management* 11: 76-84. DOI: 10.1111/jfr3.12269

- Craig, H., Gordon, L. I., 1965, Deuterium and oxygen 18 variations in the ocean and the marine atmosphere. In: *Stable Isotopes in Oceanographic Studies and Paleotemperatures*, Consiglio nazionale delle ricerche, Laboratorio di geologia nucleare, Pisa.
- 905 Dawson, J.J.C., Soulsby, C., Tetzlaff, D., Hrachowitz, M., Dunn, S.M., Malcolm, I.A., 2008. Influence of hydrology and seasonality on DOC exports from three contrasting upland catchments. *Biogeochemistry* 90: 93-113. DOI: 10.1007/s10533-008-9234-3
- Deary, H., Warren, C.R., 2017. Divergent visions of wildness and naturalness in a storied landscape: Practices and discourses of rewilding in Scotland's wild places. *Journal of Rural Studies* 54: 211-222. DOI: 10.1016/j.jrurstud.2017.06.019
- 910 Delzon, S., Loustau, D., 2005. Age-related decline in stand water use: sap flow and transpiration in a pine forest chronosequence. *Agricultural and Forest Meteorology* 129: 105-119. DOI: 10.1016/j.agrformet.2005.01.002
- Douinot, A., Tetzlaff, D., Maneta, M., Kuppel, S., Schulte-Bisping, H., Soulsby, C., 2019. Ecohydrological modelling with ECH2O-iso to quantify forest and grassland effects on water partitioning and flux ages. *Hydrological Processes* 33: 2174-2191.
- 915 DOI: 10.1002/hyp.13480
- Du, E., Link, T.E., Wei, L., Marshall, J.D., 2016. Evaluating hydrologic effects of spatial and temporal patterns of forest canopy change using numerical modelling. *Hydrological Processes* 30: 217-231. DOI: 10.1002/hyp.10591
- Ellison, D., Morris, C.E., Locatelli, B., Sheil, D., Cohen, J., Murdiyarso, D., Gutierrez, V., Van Noordwijk, M., Creed, I.F., Pokorny, J. and Gaveau, D., Spracklen, D.V., Tobella, A.B., Ilstedt, U., Teuling, A.J., Gebrehiwot, S.G., Sands, D.C., Muys, B., Verbist, B., Springgay, E., Sugandi, Y., Sullivan, C.A., 2017. Trees, forests and water: Cool insights for a hot world. *Global Environmental Change* 43: 51-61. DOI: 10.1016/j.gloenvcha.2017.01.002
- 920 Falkenmark, M., Rockström, J., 2006. The new blue and green water paradigm: Breaking new ground for water resources planning and management. *Journal of Water Resources Planning and Management* 132: 129-132. DOI: 10.1061/(ASCE)0733-9496(2006)132:3(129)
- 925 Falkenmark, M. and Rockström, J., 2010. Building water resilience in the face of global change: From a blue-only to a green-blue water approach to land-water management. *Journal of Water Resources Planning and Management* 136: 606-610. DOI: 10.1061/(ASCE)WR.1943-5452.0000118
- Farley, K.A., Jobbagy, E.G., Jackson, R.B., 2005. Effects of afforestation on water yield: a global synthesis with implications for policy. *Global Change Biology* 11: 1565-1576. DOI: 10.1111/j.1365-2486.2005.01011.x
- 930 Fatichi, S., Pappas, C., Ivanov, V.Y., 2016a. Modeling plant-water interactions: an ecohydrological overview from the cell to the global scale. *WIREs Water* 3: 327-368. DOI: 10.1002/wat2.1125
- [Fatichi, S., Vivoni, E.R., Ogden, F.L., Ivanov, V.Y., Mirus, B., Gochis, D., Downer, C.W., Camporese, M., Davison, J.H., Ebel, B., Jones, N., Kim, J., Mascaro, G., Niswonger, R., Restrepo, P., Rigon, R., Shen, C., Sulis, M., Tarboton, D., 2016b. An overview of current applications, challenges, and future trends in distributed process-based models in hydrology. *Journal of Hydrology* 537: 45-60. DOI: 10.1016/j.jhydrol.2016.03.026](#)
- 935 [DOI: 10.1016/j.jhydrol.2016.03.026](#)

- Fennell, J., Geris, J., Wilkinson, M.E., Daalmans, R. and Soulsby, C., 2020. Lessons from the 2018 drought for management of local water supplies in upland areas: A tracer-based assessment. *Hydrological Processes* 34(22): 4190-4210. DOI: 10.1002/hyp.13867
- 940 Filoso, S., Bezerra, M.O., Weiss, K.C.B., Palmer, M.A., 2017. Impacts of forest restoration on water yield: A systematic review. *PLOS One* 12: e0183210. DOI: 10.1371/journal.pone.0183210
- Forestry Commission Scotland, 2010. *The right tree in the right place: Planning for forestry and woodlands*. Edinburgh: Forestry Commission Scotland.
- Gash, J.H.C., Stewart, J.B., 1977. The evaporation from Thetford Forest during 1975. *Journal of Hydrology* 35: 385-396.
- 945 Gillefalk, M., Tetzlaff, D., Hinkelmann, R., Kuhlemann, L.M., Smith, A., Meier, F., Maneta, M.P., Soulsby, C., 2021. Quantifying the effects of urban green space on water partitioning and ages using an isotope-based ecohydrological model. *Hydrology and Earth System Sciences*-25: 3635-3652 *Discussions*. DOI: [10.5194/hess-25-3635-2021](https://doi.org/10.5194/hess-25-3635-2021) [10.5194/hess-2020-640](https://doi.org/10.5194/hess-2020-640)
- [Glover, R., Soulsby, C., Fryer, R., Birkel, C., Malcolm, I. A., 2020. Quantifying the relative importance of stock level, river temperature and discharge on the abundance of juvenile Atlantic salmon \(*Salmo salar*\). *Ecohydrology* 13: e2231. DOI: 10.1002/eco.2231](https://doi.org/10.1002/eco.2231)
- 950 [10.1002/eco.2231](https://doi.org/10.1002/eco.2231)
- Gupta, H.V., Kling, H., Yilmaz, K.K., Martinez, G.F., 2009. Decomposition of the mean squared error and NSE performance criteria: Implications for improving hydrological modelling. *Journal of Hydrology* 377: 80-91. DOI: 10.1016/j.jhydrol.2009.08.003
- [Holmes, T., Stadnyk, T., Kim, S.J., Asadzadeh, M., 2020. Regional calibration with isotope tracers using a spatially distributed model: A comparison of methods. *Water Resources Research* 56: e2020WR027447. DOI: 10.1029/2020WR027447](https://doi.org/10.1029/2020WR027447)
- 955 [10.1029/2020WR027447](https://doi.org/10.1029/2020WR027447)
- Iacob, O., Brown, I., Rowan, J., 2017. Natural flood management, land use and climate change trade-offs: the case of Tarland catchment, Scotland. *Hydrological Sciences Journal* 62: 1931-1948. DOI: 10.1080/02626667.2017.1366657
- Johnson, R.C., 1990. The interception, throughfall and stemflow in a forest in Highland Scotland and the comparison with other upland forests in the UK. *Journal of Hydrology* 118: 281-287. DOI: 10.1016/0022-1694(90)90263-W
- 960 Kleine, L., Tetzlaff, D., Smith, A., Wang, H., Soulsby, C., 2020. Using water stable isotopes to understand evaporation, moisture stress, and re-wetting in catchment forest and grassland soils of the summer drought of 2018. *Hydrological and Earth System Sciences* 24: 3737-3752. DOI: 10.5194/hess-24-3737-2020
- Knighton, J., Kuppel, S., Smith, A., Soulsby, C., Sprenger, M., Tetzlaff, D., 2020. Using isotopes to incorporate tree water storage and mixing dynamics into a distributed ecohydrological modelling framework. *Ecohydrology* 13: e2201. DOI: 10.1002/eco.2201
- 965 [Krause, P., Boyle, D.P., Bäse, F., 2005. Comparison of different efficiency criteria for hydrological model assessment. *Advances in Geosciences* 5: 89-97. DOI: 10.5194/adgeo-5-89-2005](https://doi.org/10.5194/adgeo-5-89-2005)
- Kuppel, S., Tetzlaff, D., Maneta, M.P., Soulsby, C., 2018a. Ech2O-iso 1.0: water isotopes and age tracking in a process-based, distributed ecohydrological model. *Geoscientific Model Development* 11: 3045-3069. DOI: 10.5194/gmd-11-3045-2018

Formatted: Font: Italic

- 970 Kuppel, S., Tetzlaff, D., Maneta, M.P., Soulsby, C., 2018b. What can we learn from multi-data calibration of a process-based
ecohydrological model? *Environmental Modelling and Software* 101: 301-316. DOI: 10.1016/j.envsoft.2018.01.001
- Kuppel, S., Tetzlaff, D., Maneta, M.P., Soulsby, C., 2020. Critical Zone Storage Controls on the Water Ages of
Ecohydrological Outputs. *Geophysical Research Letters* 47: e2020GL088897. DOI: 10.1029/2020GL088897
- Langan, S.J., Wade, A.J., Smart, R.P., Edwards, A.C., Soulsby, C., Billett, M.F., Jarvie, H.P., Cresser, M.S., Owen, R., Ferrier,
975 R.C., 1997. The prediction and management of water quality in a relatively unpolluted major Scottish catchment: current issues
and experimental approaches. *Science of the Total Environment* 194/195: 419-435. DOI: 10.1016/S0048-9697(96)05380-6
- Laitakari, E., 1927. Männyn juuristo. Morfologinen tutkimus. Summary: The root system of pine (*Pinus sylvestris*). A
morphological investigation. *Acta Forestalia Fennica* 33. 379p.
- Legates, D.R., McCabe, G.J., 1999. Evaluating the use of "goodness-of-fit" measures in hydrologic and hydroclimatic model
980 validation. *Water Resources Research* 35: 233-241.
- Makkonen, K., Helmisääri, H-S., 2001. Fine root biomass and production in Scots pine stands in relation to stand age. *Tree
Physiology* 21: 193-198. DOI: 10.1093/treephys/21.2-3.193
- Maneta, M.P., Silverman, N.L., 2013. A spatially distributed model to simulate water, energy, and vegetation dynamics using
information from regional climate models. *Earth Interactions* 17: Paper No 11. DOI: 10.1175/2012EI000472.1
- 985 Manoli, G., Mejjide, A., Huth, N., Knohl, A., Kosugi, Y., Burlando, P., Ghazoul, J., Faticchi, S., 2019. Ecohydrological changes
after tropical forest conversion to oil palm. *Environmental Research Letters* 13: 064035.
- Marc, V., Robinson, M., 2007. The long-term water balance (1972-2004) of upland forestry and grassland at Plynlimon, mid-
Wales. *Hydrology and Earth System Sciences* 11: 44-60. DOI: 10.5194/hess-11-44-2007
- Marsh, T., Kirby, C., Muchan, K., Barker, L., Henderson, E., Hannaford, J., 2016. The winter floods of 2015/16 in the UK.
990 Centre for Ecology and Hydrology. Available from: <https://www.ceh.ac.uk/sites/default/files/2015-01/6%20Winter%20Floods%20report%20Hi%20Res.pdf>
- Mason, W.L., Hampson, A., Edwards, C., 2004. Managing the Pinewoods of Scotland. Edinburgh: Forestry Commission.
- McDonnell, J.J., Beven, K., 2014. Debates – the future of hydrological sciences: a (common) path forward? A call to action
995 aimed at understanding velocities, celerities and residence time distributions of the headwater hydrograph. *Water Resources
Research* 50: 5342–5350. DOI: 10.1002/2013WR015141
- McHaffie, H., Legg, C.J., Worrell, R., Cowie, N., Amphlett, A., 2002. Scots pine growing on forested mires in Abernethy
Forest, Strathspey, Scotland. *Botanical Journal of Scotland* 54: 209-219. DOI: 10.1080/03746600208685038
- Mein, R.G., Larson, C.L., 1973. Modeling infiltration during a steady rain. *Water Resources Research* 9: 384-394. DOI:
10.1029/WR009i002p00384
- 1000 Moir, H.J., Soulsby, C., Youngson, A., 1998. Hydraulic and sedimentary characteristics of habitat utilized by Atlantic salmon
for spawning in the Girnock Burn, Scotland. *Fisheries Management and Ecology* 5: 241-254. DOI: 10.1046/j.1365-
2400.1998.00105.x

- Morris, M.D., 1991. Factorial sampling plans for preliminary computational experiments. *Technometrics* 33: 161-174. DOI: 10.1080/00401706.1991.10484804
- 1005 Navarro L.M., Pereira H.M., 2015. Rewilding abandoned landscapes in Europe. In: Henrique P., Laetitia N., (eds.) *Rewilding European Landscapes*. Berlin: Springer.
- Neill, A.J., Tetzlaff, D., Strachan, N.J.C., Soulsby, C., 2019. To what extent does hydrological connectivity control dynamics of faecal indicator organisms in streams? Initial hypothesis testing using a tracer-aided model. *Journal of Hydrology* 570: 423-435. DOI: 10.1016/j.jhydrol.2018.12.066
- 1010 [Neill, A.J., Tetzlaff, D., Strachan, N.J.C., Hough, R.L., Avery, L.M., Maneta, M.P., Soulsby, C., 2020. An agent-based model that simulates the spatio-temporal dynamics of sources and transfer mechanisms contributing faecal indicator organisms to streams. Part 2: Application to a small agricultural catchment. *Journal of Environmental Management* 270: 110905. DOI: 10.1016/j.jenvman.2020.110905](#)
- Nippgen, F., McGlynn, B.L., Emanuel, R.E., 2015. The spatial and temporal evolution of contributing areas. *Water Resources Research* 51: 4550-4573. DOI: 10.1002/2014WR016719.
- 1015 Parlane, S., Summers, R.W., Cowie, N.R., van Gardingen, P.R., 2006. Management proposals for bilberry in Scots Pine woodland. *Forest Ecology and Management* 222: 272-278. DOI: 10.1016/j.foreco.2005.10.032
- Peterson, T.J., Western, A.W., 2014. Multiple hydrological attractors under stochastic daily forcing: 1. Can multiple attractors exist? *Water Resources Research* 50: 2993-3009. DOI: 10.1002/2012WR013003
- 1020 Peterson, T.J., Argent, R.M., Western, A.W., Chiew, F.H.S., 2009. Multiple stable states in hydrological models: An ecohydrological investigation. *Water Resources Research* 45: W03406. DOI: 10.1029/2008WR006886
- Peng, H., Tague, C., Jia, Y., 2016. Evaluating the eco-hydrologic impacts of reforestation in the Loess Plateau, China, using an eco-hydrological model. *Ecohydrology* 9: 498-513. DOI: 10.1002/eco.1652
- Perino, A., Pereira, H.M., Navarro, L.M., Fernández, N., Bullock, J.M., Ceaușu, S., Cortés-Avizanda, A., van Klink, R., 1025 Kuemmerle, T., Lomba, A. and Pe'er, G., Plieninger, T., Benayas, J.M.R., Sandom, C.J., Svenning, J., Wheeler, H.C., 2019. Rewilding complex ecosystems. *Science* 364 (6438). DOI: 10.1126/science.aav5570
- Perry, T.D., Jones, J.A., 2017. Summer streamflow deficits from regenerating Douglas-fir forest in the Pacific Northwest, USA. *Ecohydrology* 10: e1790. DOI: 10.1002/eco.1790
- Rands, M.R., Adams, W.M., Bennun, L., Butchart, S.H., Clements, A., Coomes, D., Entwistle, A., Hodge, I., Kapos, V., 1030 Scharlemann, J.P. and Sutherland, W.J., Vira, B., 2010. Biodiversity conservation: challenges beyond 2010. *Science* 329 (5997): 1298-1303. DOI: 10.1126/science.1189138
- Robinson, M., 1998. 30 years of forest hydrology changes at Coalburn: water balance and extreme flows. *Hydrology and Earth System Sciences* 2: 233-238. DOI: 10.5194/hess-2-233-1998
- Rodriguez-Iturbe, I., 2000. Ecohydrology: A hydrological perspective of climate-soil-vegetation dynamics. *Water Resources Research* 36: 3-9. DOI: 10.1029/1999WR900210
- 1035

Rudel, T.K., Meyfroidt, P., Chazdon, R., Bongers, F., Sloan, S., Grau, H.R., Van Holt, T., Schneider, L., 2020. Whither the forest transition? Climate change, policy responses, and redistributed forests in the twenty-first century. *Ambio* 49: 74-84. DOI: 10.1007/s13280-018-01143-0

Schaefli, B., Gupta, H.V., 2007. Do Nash values have value? *Hydrological Processes* 21: 2075-2080. DOI: 10.1002/hyp.6825

1040 ~~Scheliga, B., Tetzlaff, D., Nuetzmann, G., Soulsby, C., 2019. Assessing runoff generation in riparian wetlands: monitoring groundwater-surface water dynamics at the micro-catchment scale. *Environmental Monitoring and Assessment* 191: 116. DOI: 10.1007/s10661-019-7237-2~~

Scott, D.F., Prinsloo, F.W., 2008. Longer-term effects of pine and eucalypt plantations on streamflow. *Water Resources Research* 44: W00A08. DOI: 10.1029/2007WR006781

1045 Segura, C., Bladon, K.D., Hatten, J.A., Jones, J.A., Cody Hale, V., Ice, G.G., 2020. Long-term effects of forest harvesting on summer low flow deficits in the Coast Range of Oregon. *Journal of Hydrology* 585: 124749. DOI: 10.1016/j.jhydrol.2020.124749

Seibert, J., van Meerveld, H.J.I., 2016. Hydrological change modeling: Challenges and opportunities. *Hydrological Processes* 30: 4966-4971. DOI: 10.1002/hyp.10999

1050 Simeone, C., Maneta, M. P., Holden, Z.A., Sapes, G., Sala, A., Dobrowski, S.Z. (2018). Coupled ecohydrology and plant hydraulics modeling predicts ponderosa pine seedling mortality and lower treeline in the US Northern Rocky Mountains. *New Phytologist* 221:1814-1830. -DOI: 10.1111/nph.15499

Smith, A., Tetzlaff, D., Laudon, H., Maneta, M., Soulsby, C., 2019. Assessing the influence of soil freeze-thaw cycles on catchment water storage-flux-age interactions using a tracer-aided ecohydrological model. *Hydrology and Earth System Sciences* 23: 3319-3334. DOI: 10.5194/hess-23-3319-2019

1055 Smith, A., Tetzlaff, D., Kleine, L., Maneta, M.P., Soulsby, C., 2020. Isotope-aided modelling of ecohydrologic fluxes and water ages under mixed land use in Central Europe: The 2018 drought and its recovery. *Hydrological Processes* 34: 3406-3425. DOI: 10.1002/hyp.13838

1060 ~~Smith, A., Tetzlaff, D., Kleine, L., Maneta, M., Soulsby, C., 2021. Quantifying the effects of land use and model scale on water partitioning and water ages using tracer-aided ecohydrological models. *Hydrology and Earth Systems Science* 25: 2239-2259. DOI: 10.5194/hess-25-2239-2021~~

SNH, 2016. Deer Management in Scotland: Report to the Scottish Government from Scottish National Heritage 2016. Retrieved from: <http://www.snh.org.uk/pdfs/publications/corporate/DeerManReview2016.pdf>

1065 Soheir, H., Farges, J-L., Piet-Lahanier, H., 2014. Improvement of the representativity of the Morris Method for air-launch-to-orbit separation. *IFAC Proceedings Volumes* 47(3): 7954-7959. DOI: 10.3182/20140824-6-ZA-1003.01968

Soulsby C., Birkel C., Geris J., Dick J., Tunaley, C., Tetzlaff, D., 2015. Stream water age distributions controlled by storage dynamics and non-linear hydrologic connectivity: modelling with high resolution isotope data. *Water Resources Research* 51: 7759-7776. DOI: 10.1002/2015WR017888

- Soulsby, C., Bradford, J., Dick, J., McNamara, J.P., Geris, J., Lessels, J., Blumstock, M., Tetzlaff, D., 2016. Using geophysical surveys to test tracer-based storage estimates in headwater catchments. *Hydrological Processes* 30: 4434-4445. DOI: 10.1002/hyp.10889
- 1070 Soulsby, C., Dick, J., Scheliga, B., Tetzlaff, D., 2017. Taming the flood – How far can we go with trees? *Hydrological Processes* 31: 3122-3126. DOI: 10.1002/hyp.11226
- Sprenger, M., Tetzlaff, D., Tunaley, C., Dick, J., Soulsby, C., 2017. Evaporative fractionation in a peatland drainage network affects stream water isotope composition. *Water Resources Research* 53: 851-866. DOI: 10.1002/2016WR019258
- 1075 Sprenger, M., Stumpp, C., Weiler, M., Aeschbach, W., Allen, S.T., Benettin, P., Dubbert, M., Hartmann, A., Hrachowitz, M., Kirchner, J.W. and McDonnell, J.J., Orłowski, N., Penna, D., Pfahl, S., Rinderer, M., Rodriguez, N., Schmidt, M., Werner, C., 2019. The demographics of water: A review of water ages in the critical zone. *Reviews of Geophysics* 57(3): 800-834. DOI: 10.1029/2018RG000633
- 1080 Steven, H.M., Carlisle, A., 1959. *The Native Pinewoods of Scotland*. Edinburgh: Oliver and Boyd.
- Stewart, J.B., 1977. Evaporation from the wet canopy of a pine forest. *Water Resources Research* 13: 915-921. DOI: 10.1029/WR013i006p00915
- [Stewart, M. K., Morgenstern, U., McDonnell, J. J., 2010. Truncation of stream residence time: How the use of stable isotopes has skewed our concept of streamwater age and origin. *Hydrological Processes* 24: 1646–1659. DOI: 10.1002/hyp.7576](#)
- 1085 Stockinger, M.P., Bogena, H.R., Lücke, A., Dieckkrüger, D., Weiler, M., Vereecken, H., 2014. Seasonal soil moisture patterns: Controlling transit time distributions in a forested headwater catchment. *Water Resources Research* 50: 5270-5289.
- Summers, R.W., 2018. *Abernethy Forest: The History and Ecology of an Old Scottish Pinewood*. RSPB: Inverness.
- Summers, R.W., Proctor, R., Raistrick, P., Taylor, S., 1997. The structure of Abernethy Forest, Strathspey, Scotland. *Botanical Journal of Scotland* 49: 39-55. DOI: 10.1080/03746609708684851
- 1090 Summers, R.W., Wilkinson, N.I., Wilson, E.R., 2008. Age structure and history of stand types of *Pinus sylvestris* in Abernethy Forest, Scotland. *Scandinavian Journal of Forest Research* 23: 28-37. DOI: 10.1080/02827580701646513
- Taylor, K., Rowland, A.P., Jones, H.E., 2001. *Molinia caerulea* (L.) Moench. *Journal of Ecology* 89: 126-144. DOI: 10.1046/j.1365-2745.2001.00534.x
- Tetzlaff, D., Soulsby, C., Waldron, S., Malcolm, I.A., Bacon, P.J., Dunn, S.M., Lilly, A., Youngson, A.F., 2007.
- 1095 Conceptualization of runoff processes using a geographical information system and tracers in a nested mesoscale catchment. *Hydrological Processes* 21: 1289-1307. DOI: 10.1002/hyp.6309
- Tetzlaff, D., Birkel, C., Dick, J., Geris, J., Soulsby, C., 2014. Storage dynamics in hydrogeological units control hillslope connectivity, runoff generation, and the evolution of catchment transit time distributions. *Water Resources Research* 50: 969-985. DOI: 10.1002/2013WR014147
- 1100 Thomas, H.J.D., Paterson, J.S., Metzger, M.J., Sing, L., 2015. Towards a research agenda for woodland expansion in Scotland. *Forest Ecology and Management* 349: 149-161. DOI: 10.1016/j.foreco.2015.04.003

Turetsky, M.R., Benscoter, B., Page, S., Rein, G., van der Werf, G., Watts, A., 2015. Global vulnerability of peatlands to fire and carbon loss. *Nature Geoscience* 8: 11-14. DOI: [10.1038/ngeo2325](https://doi.org/10.1038/ngeo2325)

1105 Turnbull, L., Wainwright, J., 2019. From structure to function: Understanding shrub encroachment in drylands using hydrological and sediment connectivity. *Ecological Indicators* 98: 608-618. DOI: [10.1016/j.ecolind.2018.11.039](https://doi.org/10.1016/j.ecolind.2018.11.039)

Wang, H., Tetzlaff, D., Soulsby, C., 2018. Modelling the effects of land cover and climate change on soil water partitioning in a boreal headwater catchment. *Journal of Hydrology* 558: 520-531. DOI: [10.1016/j.jhydrol.2018.02.002](https://doi.org/10.1016/j.jhydrol.2018.02.002)

[Werritty, A., Sugden, D., 2012. Climate change and Scotland: Recent trends and impacts. *Earth and Environmental Science Transactions of the Royal Society of Edinburgh* 103\(2\): 133-147. DOI:10.1017/S1755691013000030](#)

1110 White, M.A., Thornton, P.E., Running, S.W., Nemani, R.R., 2000. Parameterization and Sensitivity Analysis of the BIOME-BGC Terrestrial Ecosystem Model: Net Primary Production Controls. *Earth Interactions* 4: Paper No 3. DOI: [10.1175/1087-3562\(2000\)004<0003:PASAOT>2.0.CO;2](https://doi.org/10.1175/1087-3562(2000)004<0003:PASAOT>2.0.CO;2)

Wilson, S., McG., 2015. *The Native Woodlands of Scotland: Ecology, Conservation and Management*. Edinburgh : Edinburgh University Press.

1115 zu Ermgassen, S.O.S.E., McKenna, T., Gordon, J., Willcock, S., 2018. Ecosystem service responses to rewilding: first-order estimates from 27 years of rewilding in the Scottish Highlands. *International Journal of Biodiversity Science, Ecosystem Services and Management* 14: 165-178. DOI: [10.1080/21513732.2018.1502209](https://doi.org/10.1080/21513732.2018.1502209)